The Geological Society of America
Special Paper 450
2009

Sedimentary constraints on late Quaternary lake-level fluctuations at Bear Lake, Utah and Idaho

Joseph P. Smoot
U.S. Geological Survey, MS 926A, National Center, Reston, Virginia 20192, USA

Joseph G. Rosenbaum
U.S. Geological Survey, Box 25046, MS 980, Denver Federal Center, Denver, Colorado 80225, USA

ABSTRACT

A variety of sedimentological evidence was used to construct the lake-level history for Bear Lake, Utah and Idaho, for the past ~25,000 years. Shorelines provide evidence of precise lake levels, but they are infrequently preserved and are poorly dated. For cored sediment similar to that in the modern lake, grain-size distributions provide estimates of past lake depths. Sedimentary textures provide a highly sensitive, continuous record of lake-level changes, but the modern distribution of fabrics is poorly constrained, and many ancient features have no modern analog. Combining the three types of data yields a more robust lake-level history than can be obtained from any one type alone. When smooth age-depth models are used, lake-level curves from multiple cores contain inconsistent intervals (i.e., one record indicates a rising lake level while another record indicates a falling lake level). These discrepancies were removed and the multiple records were combined into a single lake-level curve by developing age-depth relations that contain changes in deposition rate (i.e., gaps) where indicated by sedimentological evidence. The resultant curve shows that, prior to 18 ka, lake level was stable near the modern level, probably because the lake was overflowing. Between ca. 17.5 and 15.5 ka, lake level was ~40 m below the modern level, then fluctuated rapidly throughout the post-glacial interval. Following a brief rise centered ca. 15 ka (= Raspberry Square phase), lake level lowered again to 15–20 m below modern from ca. 14.8–11.8 ka. This regression culminated in a lowstand to 40 m below modern ca. 12.5 ka, before a rapid rise to levels above modern ca. 11.5 ka. Lake level was typically lower than present throughout the Holocene, with pronounced lowstands 15–20 m below the modern level ca. 10–9, 7.0, 6.5–4.5, 3.5, 3.0–2.5, 2.0, and 1.5 ka. High lake levels near or above the modern lake occurred ca. 8.5–8.0, 7.0–6.5, 4.5–3.5, 2.5, and 0.7 ka. This lake-level history is more similar to records from Pyramid Lake, Nevada, and Owens Lake, California, than to those from Lake Bonneville, Utah.

Smoot, J.P., and Rosenbaum, J.G, 2009, Sedimentary constraints on late Quaternary lake-level fluctuations at Bear Lake, Utah and Idaho, *in* Rosenbaum, J.G., and Kaufman, D.S., eds., Paleoenvironments of Bear Lake, Utah and Idaho, and its catchment: Geological Society of America Special Paper 450, p. 263–290, doi: 10.1130/2009.2450(12).

INTRODUCTION

Bear Lake in Utah and Idaho (Fig. 1) has fluctuated in size frequently in response to changing conditions of inflow and evaporation. Historically, the lake has fluctuated from a highstand at 1805.5 m above sea level (asl) numerous times since 1920 to a low level of 1799 m asl in 1936 (Dean et al., this volume). These fluctuations are a response to regional climate change (Dean et al., this volume), although some pre-historical fluctuations may also reflect physiographic changes due to stream capture or tectonism (Reheis et al., this volume). During much of the late Pleistocene, Bear Lake was fed directly by the Bear River (Dean et al., 2006; Kaufman et al., this volume), which entered the basin from the east at a location north of the present lake (Reheis et al., this volume). During that time, the lake drained back into the Bear River via channels just east of the Bear River Range (Reheis et al., this volume).

This paper uses sedimentological data to derive a radiocarbon-dated record of lake-level fluctuations for the past ~30,000 years. The data include shoreline elevations, grain-size changes, and textural comparisons. Each data type has it strengths and weaknesses. The largest obstacle to evaluating lake-level changes is establishing the ages of different types of deposits. The density and reliability of radiocarbon ages are highly variable in the various cores and outcrops. For cored sediments, ages used in this paper are radiocarbon ages that have been converted to calendar years before 1950 (cal yr B.P.) using the terrestrial calibration set of Stuiver et al. (1998). The age estimates are median probabilities (1σ errors) reported by Colman et al. (this volume).

SHORELINE DEPOSITS

Shoreline deposits provide the most direct evidence of past lake levels. These include a characteristic suite of structures or grain-size distributions that can be inferred to have been deposited within a meter or two of the water surface at the lake edge. Shoreline deposits include wave-formed beach and bar deposits and delta topsets. Such deposits range in thickness from several meters to a thin veneer overlying a wave-cut terrace.

Modern wave-formed shoreline deposits at Bear Lake range from boulder-cobble deposits to sand (Fig. 2). Unlike the shoreline deposits of oceans or very large lakes, many of the Bear Lake shoreline deposits are not very well sorted. The relatively small size of the lake results in highly variable wave energy with the coarsest grain sizes moved during storms. Former boulder shorelines are recognized by open-framework packing with layers or patches of grains sorted by size and shape (e.g., Smoot and Lowenstein, 1991) (Fig. 3A). Sandy beaches range in character from well-sorted shoreface deposits (Figs. 3B and 3C) to poorly sorted shell gravel sheets (Fig. 3D; Smoot, this volume). Gravel sheets form where the lake-floor slope is very low. Storm waves break hundreds of meters offshore in a meter or two of water, allowing only low-energy waves to reach the shoreline (Smoot, this volume). Wave-formed bars are ridges that may form many tens of meters from shore (Smoot and Lowenstein, 1991). By comparison to wave-formed bars in marine settings, the bars are formed at depths where the crests are less than a meter or two below the surface (e.g., Komar, 1998, p. 292–302). Wave-formed bars occur where the lake-floor slope is steep enough to allow larger waves to move closer to shore. The bars are pushed shoreward by storms until they become attached to the shoreline. The lakeward sides of the bars are subsequently eroded and redistributed, or they act as a new shoreface for beach deposits. The relatively small surface area of Bear Lake produces only small-scale offshore bars (tens of centimeters thick). Wave-cut terraces are erosional surfaces. Wave erosion is an initial response to rising water levels but long-term erosion is a function of sediment supply (see Komar, 1998, p. 121–129). Large terraces are commonly attributed to lake still stands (e.g., Benson, 1994; Adams and Wesnousky, 1998), but stepped terraces would be expected in a rising lake. Sediments deposited over a terrace range from a single layer of imbricated pebbles to a sediment platform several meters thick that is built into the lake. A sediment platform is deposited as a series of lakeward-dipping foresets composed of wave-sorted sediment (see Smoot and Lowenstein, 1991). Such deposits are thin within the Holocene section at Bear Lake, but some of the meters-thick Pleistocene "fan delta" deposits noted in Laabs and Kaufman (2003) may have originated in this manner.

Deltas are lakeward-thickening wedges of sediment formed at the intersection of streams or rivers and standing bodies of water (e.g., Coleman, 1981). Delta deposits in Bear Lake have two styles. Birdfoot distributaries with mouth bar deposits occur where the Bear River previously intersected the lake. Gilbert-type delta deposits (Gilbert, 1885) with well-defined delta foresets and topsets occur where sediment-laden streams debouched from canyons directly into the lake. Robertson (1978) examined the distribution of fluvial and deltaic sediments in the north end of Bear Lake Valley, and some data on delta distributions were provided by Laabs and Kaufman (2003). Colman (2006) presented seismic evidence of Pleistocene deltaic deposits in the eastern side and north end of the lake. The sedimentary characteristics of delta deposits around Bear Lake have not been studied in any detail.

Laabs and Kaufman (2003) and Reheis et al. (2005, this volume) documented evidence of shorelines in outcrops around Bear Lake. The study of Laabs and Kaufman (2003) included data from Williams et al. (1962), Robertson (1978), and McCalpin (1993). Most of the shoreline features noted in these studies are beach gravel deposits. They mention delta and fan-delta deposits, but do not indicate recognition of the topset-foreset transition, which is necessary to accurately ascertain water depth. Additional shoreline data include sandy beach deposits and shell gravels in sediment cores within the lake (Smoot, this volume). Colman (2006) recognized an erosional terrace in seismic records of the lake floor that was interpreted as a shoreline feature. The top of the terrace is at 1798 m and the base is at 1784 m elevation. Dean (this volume) described an aragonite-cemented, boulder-cobble deposit called the "rock pile" whose base is at 1786 m and top is at 1792 m. Dean (this volume) interpreted this deposit as a microbialite mound probably related to spring activity. The

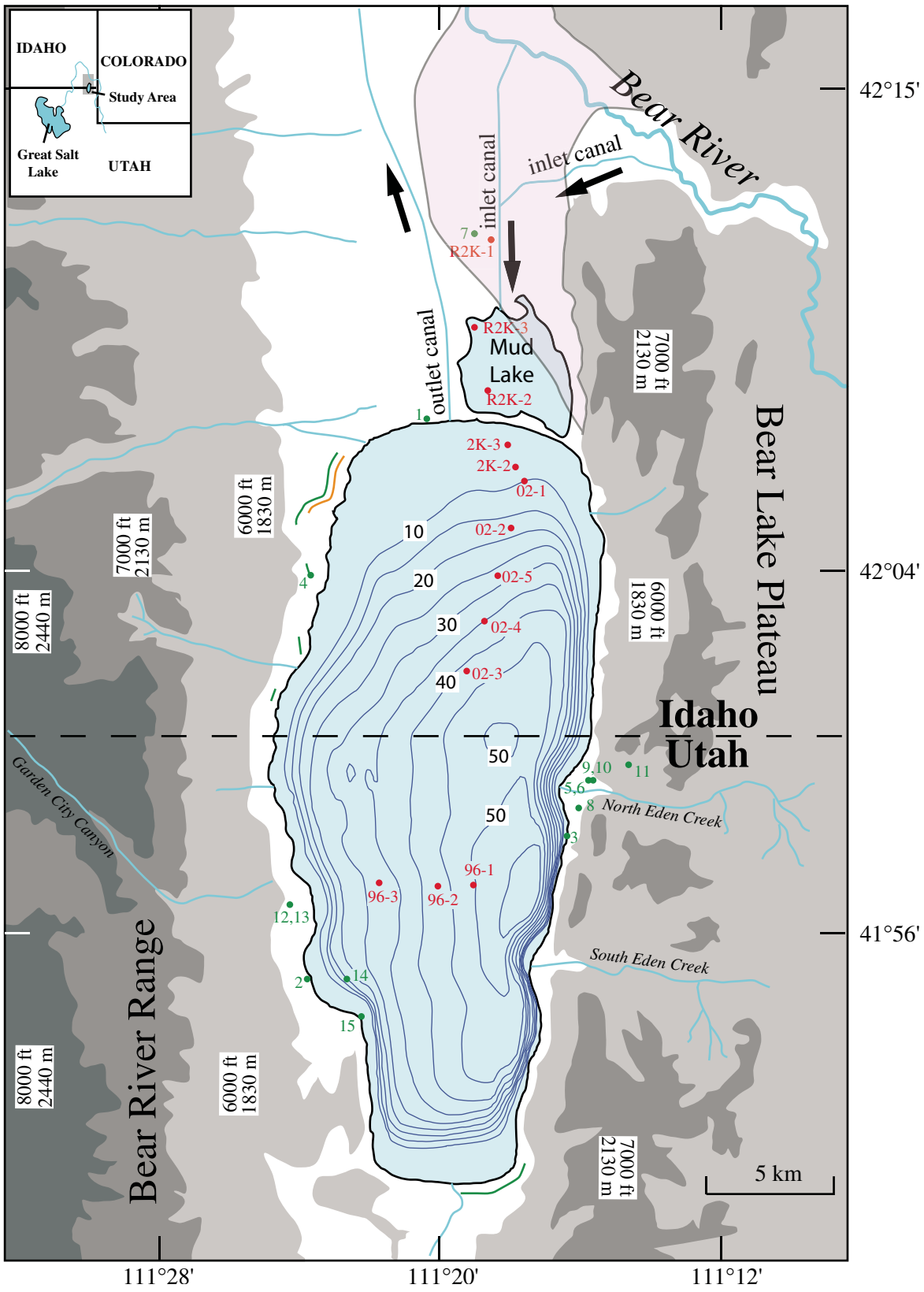

Figure 1. Map of Bear Lake at the modern highstand level (1805.5 m). Isobaths are in meters (note the absence of a 5 m contour). Land elevation contours are rounded off to the nearest 10 m. Red dots are core localities. Green dots are locations of dated shorelines, and numbers refer to samples in Table 1. Green lines show the Willis Ranch shoreline (1814 m) and the orange line shows the Garden City shoreline (1811 m). Pink area to north shows extent of Pleistocene deltaic sands from Robertson (1978). Map is modified from Laabs and Kaufman (2003). Bathymetry is from Denny and Colman (2003).

boulder descriptions are more consistent with a wave-formed shoreline or bar deposit with algal tufa buildups, similar to shoreline deposits in other lakes, such as Lake Lahontan in Nevada and California (Benson, 1994).

Wave-formed shoreline deposits are characterized by a mixture of erosion and aggregation features reflecting sediment availability, accommodation space, duration of a lake level, and changing wave energy (Adams and Wesnousky, 1998, p. 1327). The sediment that accumulates in these deposits may include material eroded from previous deposits including shells and organic material. Furthermore, the contact between the shoreline deposit and underlying deposits may be an erosional surface, and a shift of lake level may cause a former shoreline feature to be completely eroded. The net effect of these characteristics is that the age of a shoreline deposit is often uncertain. For instance, a shell gravel in core BL02-5 (Fig. 1) has white snail shells with an age of 2860 cal yr B.P. and black snail shells of apparently the same species with an age of 3520 cal yr B.P. Shells collected from the Lifton shoreline (Fig. 1) show a range of ages (8700–6400 cal yr B.P.) (Laabs and Kaufman, 2003) that suggest reworking and possible reoccupation of the same shoreline. Most shoreline ages referred to in this paper were derived from shelly material within the deposit or within adjacent finer-grained material. Similar results from multiple shells provide more confidence in the shoreline ages. Additional problems with dating shorelines are discussed later in the section on chronology.

Abundant evidence of fault movement in Bear Lake Valley (McCalpin, 1993; Colman, 2006; Reheis et al., this volume) adds to the uncertainty of shoreline elevations. McCalpin (1993) argued that 12,000-year-old shoreline deposits on the east side of the lake were probably uplifted ~8 m by fault movement. Colman (2006) noted numerous faults below the lake floor, some cutting the youngest sediment. Movement along these faults may have changed lake-floor and shoreline elevations.

Shoreline Results

The subaerial shoreline record for the past 35,000 years is relatively sparse. Deposits at 1801–1806 m asl reflect historical fluctuations of the lake. Older deposits occur between

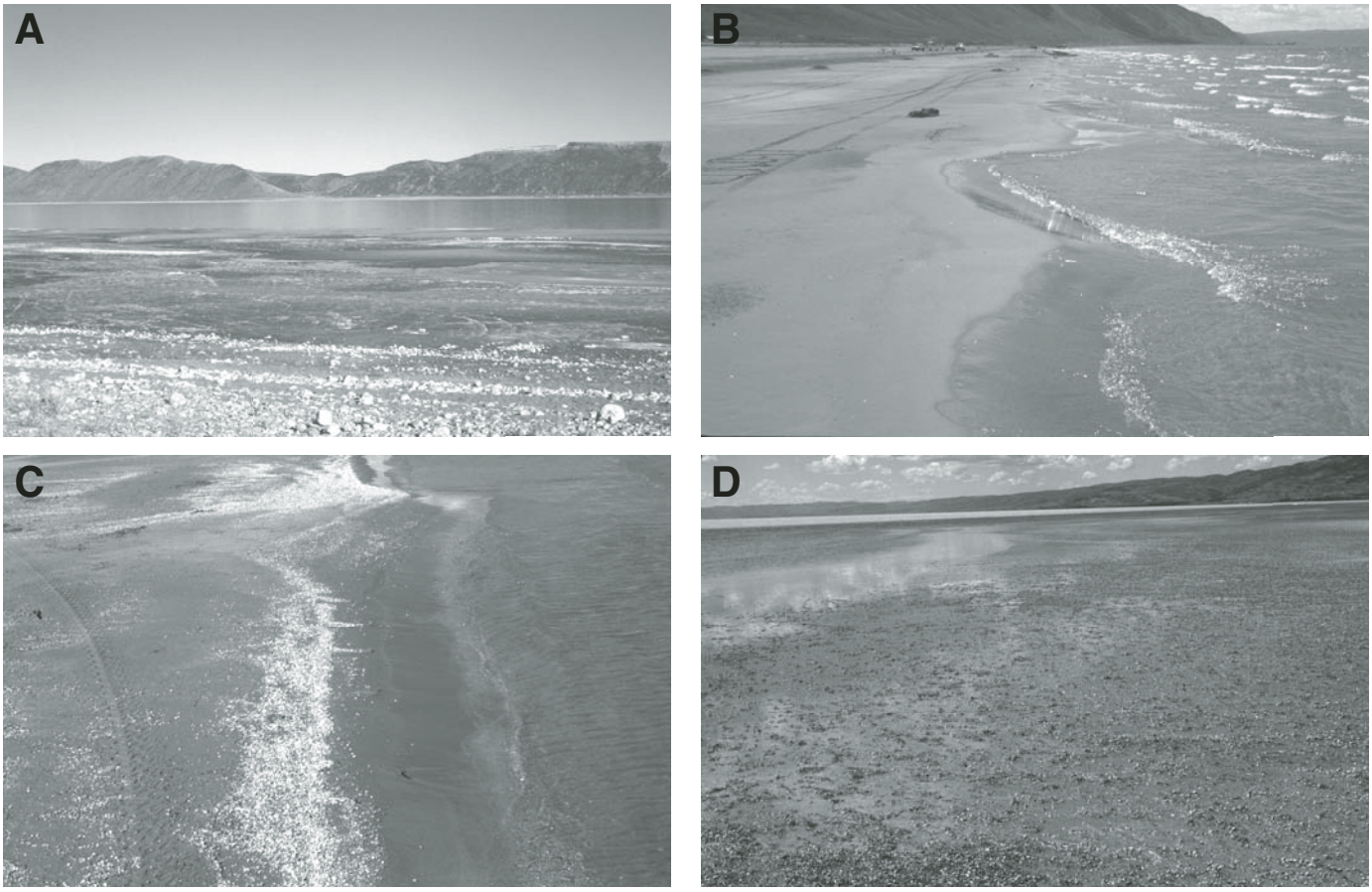

Figure 2. Modern shoreline features. (A) Boulder-cobble strandlines on west side of lake. Background shows small sand bars exposed by a recent drop in lake level. (B) Sandy shoreline on east side of lake. Note small, wave-cut terrace in background. (C) Shell-rich sandy shoreline on west side of lake. The steep shoreface is producing lakeward-dipping foresets. Note ripples underwater in front of shore. (D) Shell gravel on northeastern shore of lake. A sheet of shell gravel extends a couple of kilometers inland on the flat shoreline.

1808 and 1814 m asl and yield ages ranging from ca. 6390 to 16,300 cal yr B.P. (sources of observations and ages are in Table 1). A well-defined shoreline on the northwest side of the lake (1811 m asl), called the Garden City shoreline (Williams et al., 1962), is undated. On the west side of the lake, the deposits of the Raspberry Square highstand and the Willis Ranch shoreline occur at 1814 m asl, indicating that the lake rose to this elevation ca. 16,000 cal yr B.P. and again ca. 9200 cal yr B.P. (Table 1). The ages for these and other shorelines may be too old because of reservoir effects or reworking of shells. A number of other shoreline features on the east side of the lake occur at this elevation and higher, but correlating the features is confounded by differential uplift along faults bounding the east side of the valley (McCalpin, 1993; Laabs and Kaufman, 2003). No shoreline features above the modern lake level have been observed for the period from ca. 16,000 to 35,000 cal yr B.P. Fluvial and marsh deposits dated at 13,000–9000 cal yr B.P. in the area north of the lake suggest that the lake did not exceed the 1808 m asl shoreline and probably did not exceed 1806 m asl during that period (Laabs, 2001). Emerged beach gravel exposed on the east side of Bear Lake at Cisco Beach is dated ca. 12,000 cal yr B.P. (Laabs and Kaufman, 2003), although the extent to which the gravel has been uplifted is not known for certain.

Sublacustrine geomorphic expressions of shorelines include (1) an undated erosional bench at 1784–1798 m asl; (2) the upper surface of a delta deposit located at the northern end of the lake

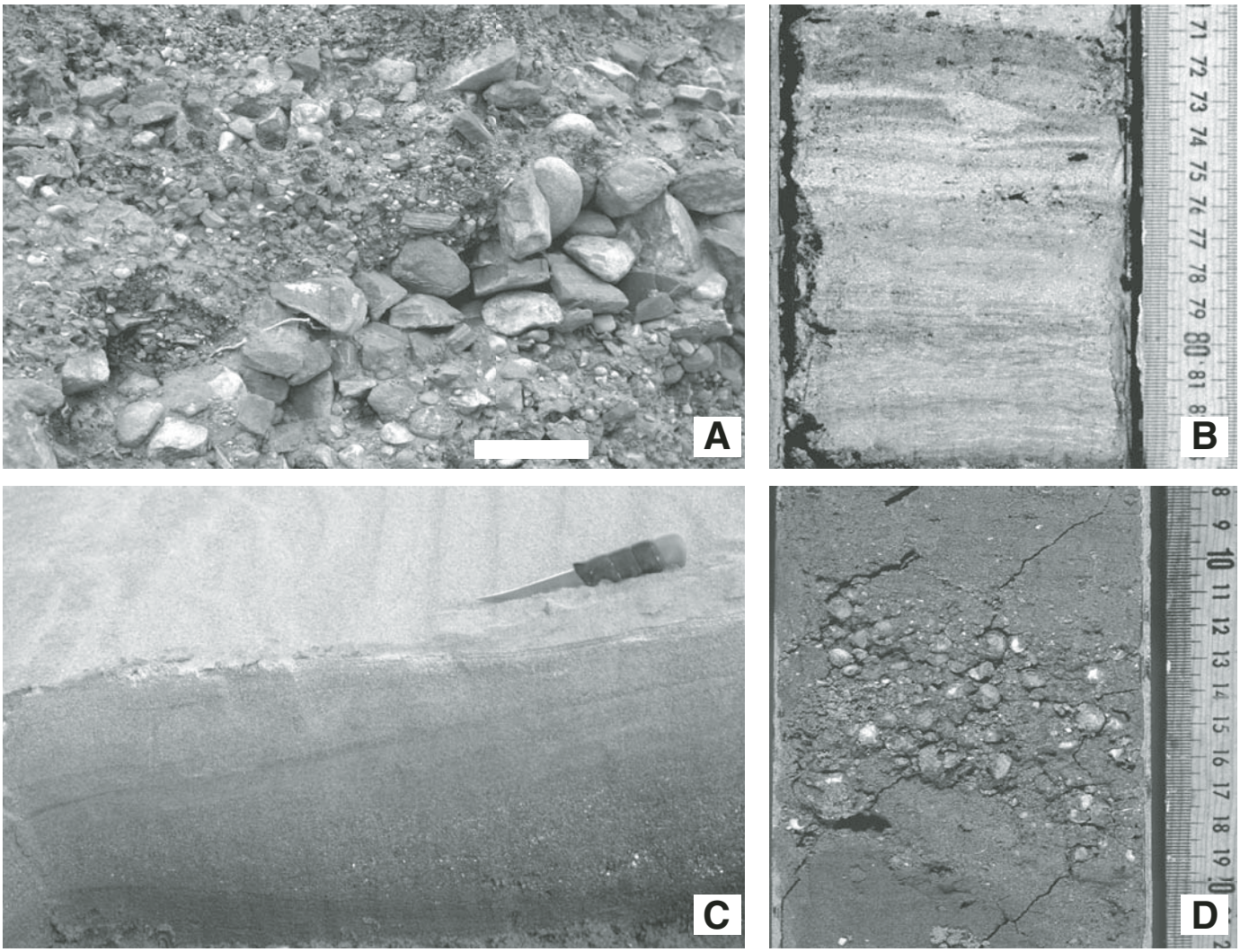

Figure 3. Cross sections of shoreline sediment. (A) Exposure of boulder-cobble strandline deposit at North Eden Canyon. Note characteristic open-framework packing of small boulders with similar sizes and shapes and abrupt transition to well-sorted gravel (matrix is infiltrated around clasts). Scale bar is 20 cm. (B) Wave-rippled sand with thin muddy partings (dark) in core BL02-5. This represents deposition in less than 5 m of water. Scale is in centimeters. (C) Beach sand in trench on west side of lake near Garden City. Shoreface sand forms lakeward-dipping planar sand beds. These overlie steep, shell-rich, lakeward-dipping foresets. Base of trench is muddy sand with wave ripples. Knife is 25 cm long. (D) Shell gravel beach deposit in core BL2K-3. The gravel is overlain and underlain by muddy sand. Scale is in centimeters.

observed on seismic profiles at 1798 m asl and having an estimated age for the overlying reflector of 35,000 yr (Colman, 2006); and (3) the boulder deposit at 1786–1792 m asl (about the same elevation as the erosional bench) known as the "rock pile" (Fig. 1). Aragonite coatings on a cobble from the boulder deposit yield ages ranging from 7470 to 3300 cal yr B.P., but these ages may be too old (Dean, this volume). Also, the boulder deposit could be much older than the aragonite coating. During a period of low lake level, bones of a mastodon were recovered from the area of a sublacustrine spring at an elevation of 1804 m asl. The bones, which yielded an age of 22,000 cal yr B.P., indicate that the spring was subaerial at that time (Laabs and Kaufman, 2003).

Cores taken in ~35 m of water or less (i.e., at or above 1770.5 m asl) contain shoreline deposits or deposits that formed at lake depths less than 5 m (Table 1). The shoreline deposits are typically shell gravels that formed as gravel sheet deposits. In the deeper cores (BL02-5, BL96-3, and BL02-4), graded sand and shell gravel layers may not be true shorelines, but probably formed in less than 5 m of water, shallow enough for waves to move the grain sizes in the layers (Smoot, this volume). Ages of these deposits are better constrained by radiocarbon dating of pollen concentrates from adjacent sediments rather than by ages from shells within the deposits (Colman et al., this volume). Core shoreline data indicate that the lake dropped as low as 1776 m asl sometime between 9800 and 9200 cal yr B.P. and ca. 2800 cal yr B.P. Lake level may also have been as low as 1779 m asl sometime between 5000 and 7000 cal yr B.P., according to shell gravel age constraints in BL96-3, BL02-4, and BL02-5 (Table 1).

TABLE 1. SHORELINE AGES AND ELEVATIONS

Location	Elevation (m asl)	Age (cal yr B.P.)	Dated material	Comments
1	1808	8090 ± 70	mollusk shell	(1) Lifton shoreline
		<6390 ± 60	charcoal	
2	1808	8540 ± 100	mollusk shell	(2) Lifton shoreline
3	1808	8780 ± 270	mollusk shells	(2) Lifton shoreline
4	1814	9220 ± 360	mollusk shells	(2) Willis Ranch shoreline
5	1814	9840 ± 130	charcoal in overlying marsh deposits	(1) North Eden Canyon fault uplift
6	1814	10,400 ± 130	charcoal in overlying marsh deposits	(3) North Eden Canyon fault uplift
7	1810	11,260 ± 50	mollusk shells	(1) Fault uplift?
8	1814	12,510 ±170	mollusk shell	(4) Cisco Beach fault uplift
9	1814	12,540 ±170	*Discus* shell	(1) North Eden Canyon fault uplift
10	1814	12,830 ± 90	*Discus* shell	(1) North Eden Canyon fault uplift
11	1830	15,150 ± 760	mollusk shell	(3) North Eden Canyon fault uplift
12	1814	16,310 ± 240	*Limnaea* shell	(1) Raspberry Square phase deposit
13	1814	16,010 ± 270	*Limnaea* and *Discus* shells	(1) Raspberry Square phase deposit
14	1786–1792	>7475 ± 40	aragonite crust	(5) Rock pile
		>2000	comparison to $\delta^{18}O$ of lake sediment	
15	1804	22,000 ± 375	mastodon bones in spring	(4)
BL2K-3	1800	3540 ± 80	shells	(6)
BL02-1	1796	>1910 ± 60	pollen	(6)
		<6180 ± 50	pollen	
		7810 ± 80	gastropod	
BL02-1	1796	>9250 ± 120	pollen	(6)
		<11,540 ± 140	pollen	
BL02-1	1796	<13,240 ± 50	pollen	(6)
		12,080 ± 240	gastropod	
BL02-2	1788	>1880 ± 50	pollen	(6)
		<25,390 ± 190	pollen	
		8360 ± 30	gastropod	
BL02-5	1779	<23,170 ± 310	pollen	(6)
		7000 ± 100	gastropod	
BL96-3	1773	>5050 ± 80	pollen	(6)
BL02-4	1771	>2780 + 50	pollen	(6)
		<5660 ± 50	pollen	
		2860 ± 70	gastropod	
		3520 ± 40	gastropod	
BL02-4	1771	>9200 + 70	pollen	(6)
		<9870 ± 40	pollen	
		10,000 ± 100	gastropod	

Note: Locations are keyed to Figure 1. ">" and "<" indicate ages in overlying and underlying sediment, respectively. Numbers in parentheses indicate source of data: 1—Reheis et al. (2005); 2—Williams et al. (1962); 3—McCalpin (1993); 4—Laabs and Kaufman (2003); 5—Dean (this volume); 6—Colman et al. (this volume). asl—above sea level.

GRAIN SIZE

The classic description of sediment distribution indicates a decrease of grain size from the margins to the center of a lake (see Hakanson and Jansson, 1983). Both stream inflow and wave-induced processes operate to segregate grain sizes in this manner. In a delta setting, the stream jet loses momentum upon intersecting the lake, which causes saltating grains to cease moving and sediment suspended by turbulence to settle (see Smith and Ashley, 1985; Nemec, 1995). The depth of wave influence on sediment size and the level of energy available are dependent upon the height and period of the waves, which are in turn dependent upon the wind stress and fetch (Johnson, 1980, Hakanson and Jansson, 1983; Rowan et al., 1992). Greater water depth requires unusually large waves to move bottom sediment, whereas in shallow water, even small, gentle waves can suspend and transport silt and clay. At a given site, changes in grain size may reflect changes in water depth. Other factors, such as changes in grain shape, variations in the lake's thermal structure, or differences in the initial concentration of suspended sediment may affect grain settling (Sturm, 1979). The correlation of decreasing grain size to depth applies only to mechanically transported sediments. Sizes of grains formed biologically (e.g., shells), or chemically (i.e., endogenic and authigenic minerals), can be independent of lake depth. For this study, grain sizes of siliciclastic material in surface samples were examined as a function of water depth and then compared with similar data from core samples.

Methods

Samples of surface sediment (upper 1.5 cm) were collected along four depth transects (Fig. 4A) and 1-cm-thick core samples were collected at 2 cm intervals from cores from sites BL02-3 and BL02-4 (Fig. 1), and at 4 cm intervals from core BL96-3 (Rosenbaum et al., this volume). The surface samples were collected with a piston corer and extruded on site to prevent mixing during transport. Each sample was treated to remove carbonate, organic material, and biogenic silica (Rosenbaum et al., this volume). The residue, consisting of siliciclastic sediment, was analyzed using a laser particle-size analyzer.

Approach and Application of Grain-Size Comparisons

Each transect of surface samples shows a progressive fining away from the shoreline (Figs. 4 and 5); however, the variation of grain size with depth is different for each transect. This implies that there is no simple relationship between water depth and grain size. Because delta input is virtually absent in the modern lake, these grain-size data were compared with mathematical models based on wave influence.

Johnson (1980) and Rowan et al. (1992) attempted to quantify the relation between lake depth and grain size using Airy wave models that relate wave height to wind speed and fetch. The wave height, wavelength, and wave celerity of an Airy wave are mutually constrained; by determining one parameter the others can be derived. Rowan et al. (1992) provided equations where the maximum possible wave height of a deep-water Airy wave (wavelength is less than four times water depth) is constrained by the maximum effective fetch (Hakanson and Jansson, 1983, p. 188–191) at any given point. For a given water depth, the bottom shear stress of that wave can be derived. Komar and Miller (1973, 1975) established formulas relating the minimum wave bottom-shear stress to movement of different grain sizes. The transport formulas assume the grains approximate quartz spheres, so they are not applicable to grains less than silt size. Combining these relationships, one can constrain the maximum depths for waves to move different grain sizes for a lake. This technique was applied to Bear Lake using a 1 km grid over the modern highstand surface area. The results were extended to shallow water using equations provided by Johnson (1980) under the assumption that the adjacent deep-water wave periods remain constant.

The results of the analysis—the maximum grain size that can be moved by the largest possible wave at each grid point—were contoured (Fig. 4A) and compared with grain sizes from each of the surface transects. For all transects, the observed median grain size in the area of sand-sized grain transport is well below the maximum, suggesting that maximum-size waves have not occurred recently. The finer grain sizes, however, are consistently coarser than the grain size predicted by the wave model. This difference is least pronounced in the northernmost transect, which is the area with lowest bottom slope. In comparison to the northernmost transect, transects over steeper bottoms show different grain-size relations to depth, with a tendency for coarser grain sizes to occur farther offshore. This observation suggests that a mechanism other than wave transport influences grain size. Gravity flows are the most likely candidate for bottom transport, explaining the association with steeper slopes. Gravity flows can be initiated by a variety of mechanisms including floods, earthquakes, and high wave activity. The evidence for this mechanism in Bear Lake is discussed below.

Sediment traps deployed in the lake during this study (Dean, this volume) collected high-Mg calcite near the surface, but mostly aragonite near the lake floor. This is best explained by the presence of subsurface gravity transport of sediment containing aragonite eroded by waves from nearshore deposits. The transport of shallow-water sediment into deeper areas of a lake is called sediment focusing (Lehman, 1975; Davis and Ford, 1982; Hilton, 1985; Blais and Kalff, 1995). The bottom slopes over many areas of the lake are well within values conducive to gravity flows (Rowan et al., 1992; Hakanson, 1995). The erosion and transport of sediments from the lake edge to the lake center is also indicated because there is little Holocene sediment in water shallower than 30 m compared with much thicker deep-water Holocene deposits (Colman, 2006; Dean et al., 2006; Smoot, this volume). Smear slides (mm-scale sample) from some sediment intervals are dominated by a single carbonate mineral phase with a characteristic crystal habit (such as 3–5 μm aragonite needles versus 7–10 μm aragonite needles) and by diatoms of one or two genera (Smoot,

this volume). In contrast, smear slides of other sediment intervals contain mixtures of different carbonate mineral phases and crystal sizes as well as highly variable mixtures of benthic and pelagic diatoms. Smoot (this volume) interpreted these latter smear slides as evidence of sediment mixing due to erosion and transport. In some closed-basin lakes, the effect of sediment focusing is exaggerated by falling lake levels (Smoot, 2003; Smoot and Benson, 2004). During the period that sediment traps were deployed and surface sampling occurred, the water level in Bear Lake was falling (Dean, this volume; Rosenbaum et al., this volume).

The depth-grain size relation of gravity-flow deposits is not easily defined and is site dependent. Therefore, those transects

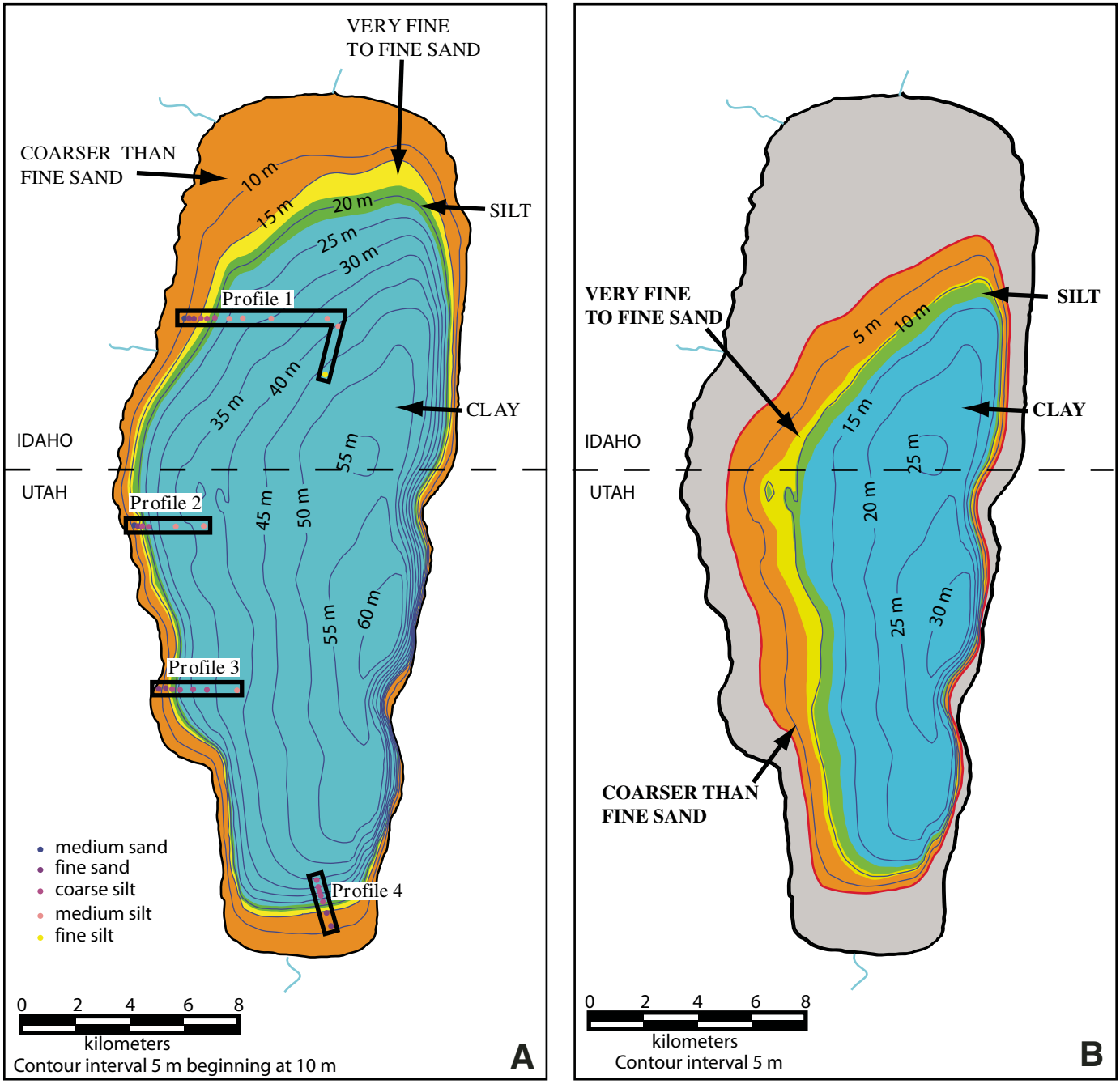

Figure 4. Maps showing maximum depth of wave transport for different grain sizes at Bear Lake. Bathymetry is from Denny and Colman (2003). (A) Model for Bear Lake at the maximum historical elevation. The collection sites of four transects of surface samples are shown with the median grain size at each locality. (B) Model for Bear Lake at a level 25 m below the historical maximum. Gray shows area of modern highstand above this lake model.

with strong indications of sediment focusing (profiles 2, 3, and 4) were considered poor candidates for modeling lake-depth changes. Median grain sizes for the northernmost transect (profile 1) are the closest to the wave model (Fig. 4A), and this transect has a similar slope to that of the core transect from the northern edge of the lake to the center. Therefore, a curve was fit to the median grain size versus depth data for profile 1 (Fig. 5). This curve was used to calculate a modeled depth for each grain-size sample from core sites BL02-3, BL02-4, and BL96-3.

The strength of this approach is that it relates past grain-size distributions to those from modern lake-bottom sediment, which can be directly related to a physical model. As long as the boundary conditions for sediment transport are similar, the technique should provide reasonable approximations of the lake depth through time. There will always be an uncertainty with respect to the influence of gravity flows in disrupting the pattern, but the slope of surface profile 1 is similar to the slopes from which the cores were taken (Fig. 4A), and the surface samples incorporate modern sediment focusing. A more subtle problem is related to changes in the wave model in response to changes in the lake size. When water level was lower than the modern level, Bear Lake was smaller and the maximum waves were smaller. Under such a scenario, the minimum depth for accumulation of sediment finer than silt is much less than for the modern Bear Lake (Fig. 4B). Therefore, modeled water depths based on modern surface samples overestimate the depth of water in a smaller lake. For a larger lake, the opposite is true, but shoreline constraints suggest that this is not a significant problem at Bear Lake because it did not have a substantially larger fetch at higher surface elevations.

The grain-size-distribution model is not applicable to times when the Bear River was transporting sediment into Bear Lake. The influx of sediment from the delta setting changes the surface-sediment distributions, particularly those of the finer sediment fractions. It is also likely that the grain-size-distribution approach will provide spurious results during periods when siliciclastic sediment not available today was reworked and mixed with the carbonate sediment. The siliclastic residue from Holocene aragonite ranges from 20% to 25% (Dean et al., 2006; Dean, this volume); siliciclastic fractions significantly greater than this range will probably distort the modeled depths. A very small Bear Lake will be more removed from the immediate mountain drainages than a larger lake. It is possible that the relative siliciclastic input from the mountains will always be finer grained in the smaller lake than in the larger lake, skewing model depths toward deeper values.

Another potential source of error in the grain-size method results from differences between surface samples and core samples. The time interval represented by a water-rich surface sample is shorter than that for a more compacted core sample of similar thickness. This disparity could create a significant problem in sediment intervals where depth changed rapidly (Fig. 6). Burrowing may have caused greater mixing in core samples, because more time was available for mixing, and mixing could include both older and younger deposits. The 1-cm-thick core samples may also include material from two very different layers (e.g., when a sample spans an erosional contact), thereby averaging contrasting grain sizes.

Grain-Size Results

The results from site BL02-3 (modern depth 43 m) indicate that lake levels were below modern lake (bml) for all but the interval from ~175 to 200 cm and another short interval at ~290 cm (Fig. 7). The model indicates that lake levels were on average 20 m bml and reached 25 m bml twice (~220 and ~250 cm). At site BL02-4 (modern depth 35 m), the model indicates that lake levels were below the modern level for all of the upper 225 cm except for intervals at ~5–10 cm and ~160–165 cm (Fig. 7). The model indicates that lake level averaged ~10 m bml and reached ~17 m bml twice (~85 and ~190 cm). The model-derived depths for the interval from ~225 cm to the base of BL02-4 are mostly at or above the modern lake level, but these results are questionable because the siliciclastic content in this interval is significantly

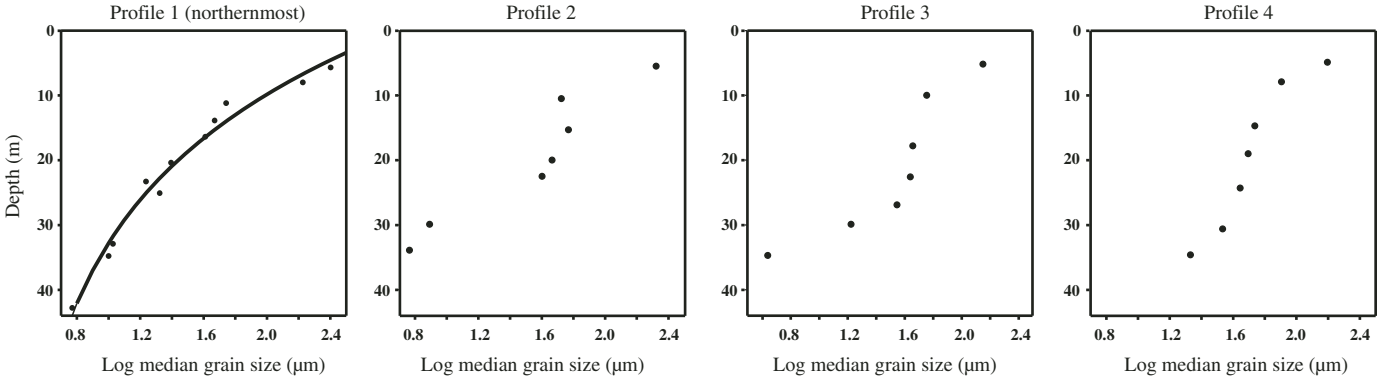

Figure 5. Log of median grain size for surface samples along the four sampling transects shown in Figure 4A. Graphs show median grain size for each sample. The curve in profile 1 was used to compute modeled lake depths shown in Figure 7. The equation for the curve is $Y = 21.4664 - 23.9725 * \ln(X - 0.3772)$ and $R^2 = 0.9800$.

higher than that of the modern lake sediments (Dean, this volume). The time significance of these intervals will be discussed in more detail following a discussion of chronology.

The siliciclastic-rich portions of BL02-4 (Fig. 7) and BL96-3 are not suitable for the lake-depth reconstruction model based on profile 1, but they do show important variability in grain size. Smoot (this volume) noted that most of the clay-sized siliciclastic sediment is rock flour rather than clay minerals throughout the siliciclastic-rich intervals. Rosenbaum et al. (this volume) and Rosenbaum and Heil (this volume) showed a correspondence between finer grain size and the content of rock material derived from the Uinta Mountains, which they interpret to be glacial flour. They interpret variations in grain size, as well as concomitant variations in magnetic properties and geochemistry, to reflect varying proportions of fine-grained glacial flour from the Uinta Mountains and coarser-grained material from the local catchment. Such variations could have arisen either from changes in input of glacial flour (due to changes in glacial activity or changes in the Bear River), or to changes in the input of local material (due to processes in and around the lake). Rosenbaum et al. (this volume), and Rosenbaum and Heil (this volume) favor an interpretation that glacial activity in the Uinta Mountains is largely responsible for the observed variations.

SEDIMENTARY TEXTURES

Sedimentary textures are manifestations of bulk-sediment grain size (as opposed to the grain size of the siliciclastic fraction described in the previous section), sorting, bedding features, other sedimentary structures, and biological or chemical components that collectively define the sediment. The sedimentary features used in this study were defined by hand-lens-scale, continuous analysis of

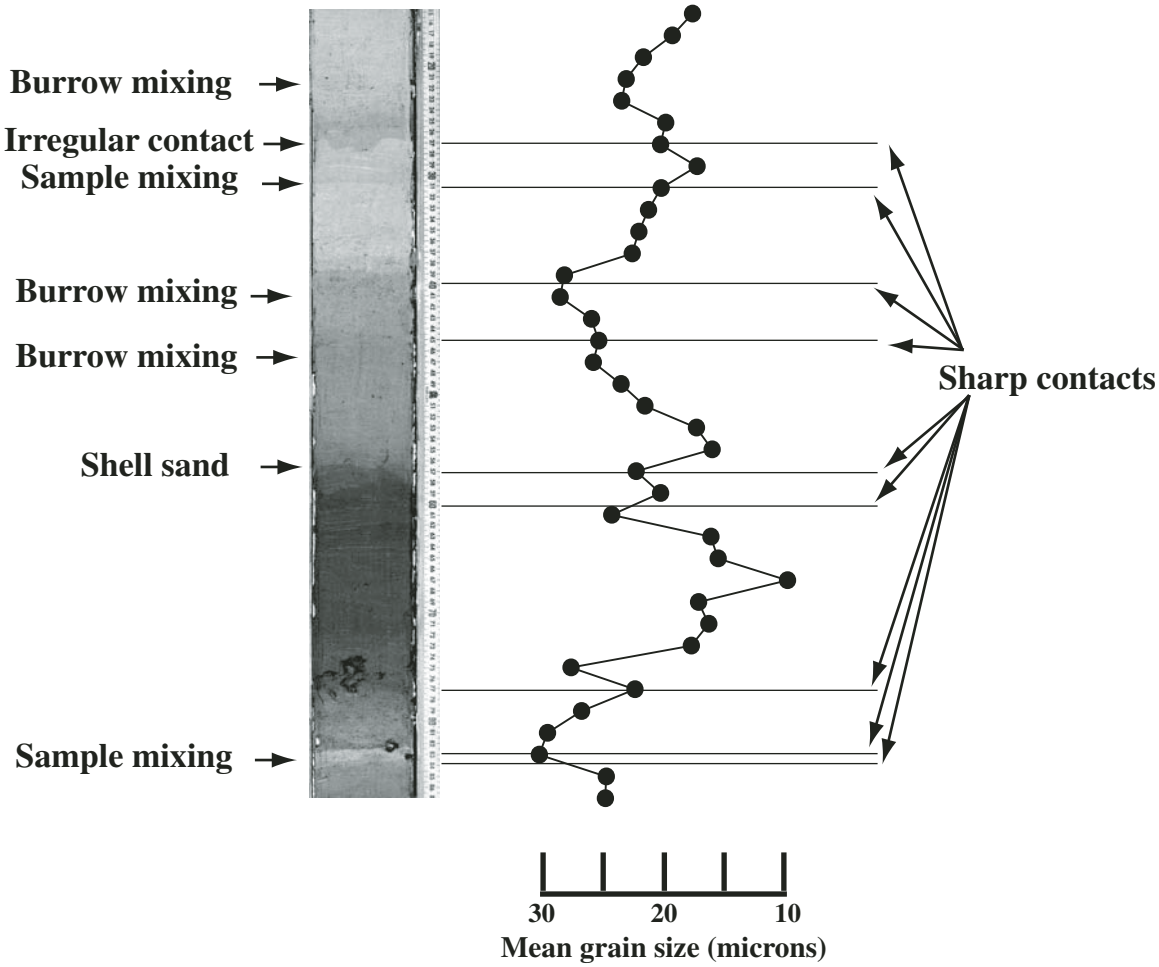

Figure 6. Median-grain-size data of siliciclastic residue plotted against sedimentary features in a segment of core BL02-4. Finer material is overlain by coarser material at numerous sharp contacts. Samples spanning these contacts average contrasting grain sizes, thereby reducing variability. Such averaging is most significant at irregular contacts and across very thin beds. Burrow mixing across sedimentary contacts also changes grain sizes from depositional values. Note that a layer composed largely of ostracode shells is medium-sand-sized, but its siliciclastic residue is medium-silt-sized. Scale is in centimeters.

all cores, X-radiography of selected cores, smear-slide petrography at irregular intervals from most cores, and SEM image analysis of selected intervals (Smoot, this volume). These analyses provide a more continuous depiction of variability than most other techniques that rely on discrete sampling, which averages properties over centimeter-thick samples. Although few sedimentary textures are absolute depth indicators, the composite distribution of textures allows one to interpret relative depth changes. Key features for constraining lake levels in Bear Lake include wave-formed structures, erosional features, grain types, sorting, root structures, and mineralogy. Additional lake-level information can be inferred from bioturbation styles and bulk grain-size distributions.

Like grain size, the formation of different types of wave-formed ripples (Figs. 8A and 8B) is linked to quantifiable wave

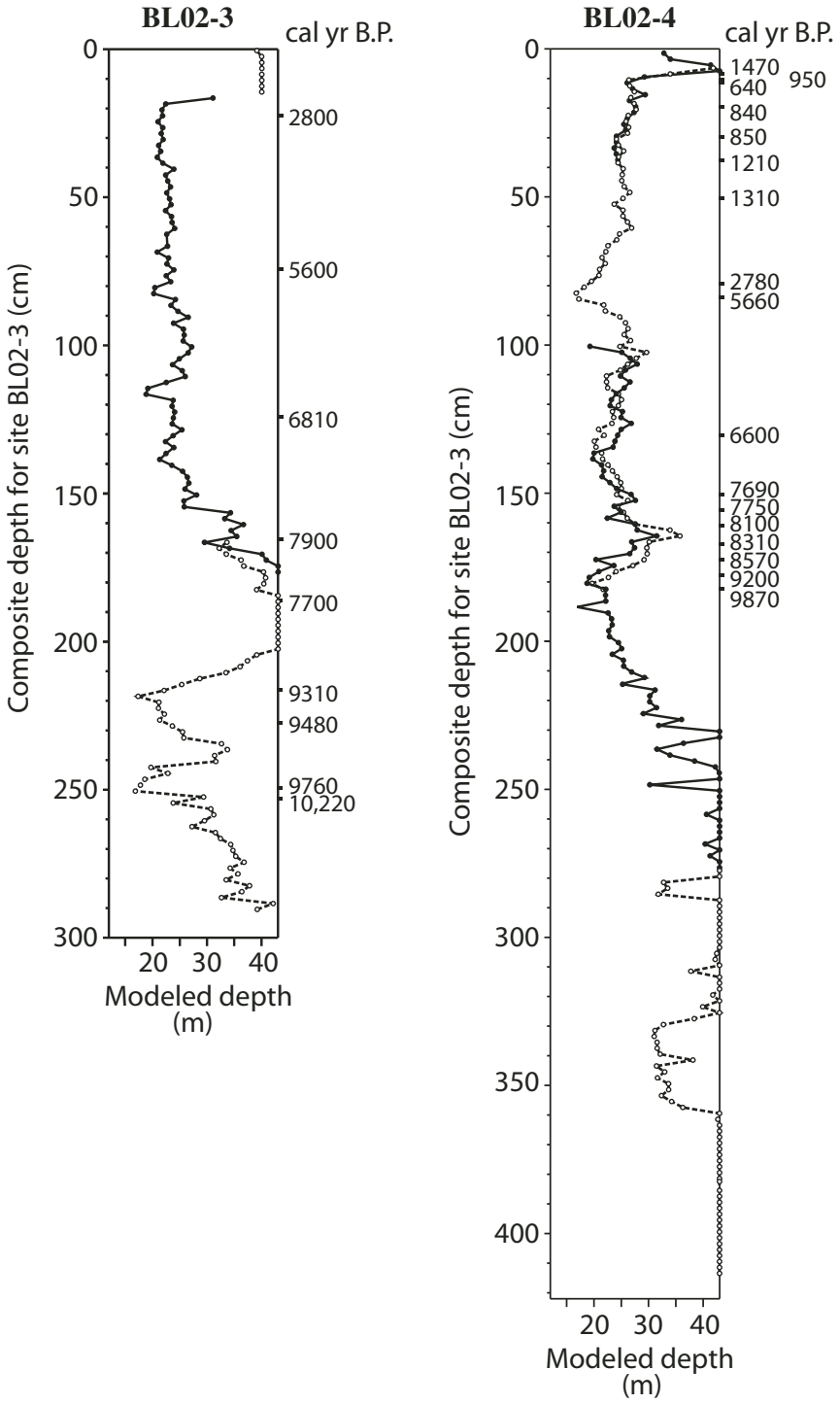

Figure 7. Modeled water depths for core sites BL02-3 and BL02-4 (Fig. 1). Depths were computed using median grain sizes of 1-cm-thick core samples and the polynomial based on the depth distribution of grain sizes of surface samples on profile 1 (Fig. 5). Samples with grain sizes that indicated depths greater than 43 m (the maximum depth for profile 1) were assigned model depths of 43 m. The sampled sections were acquired in overlapping core segments that are indicated by alternating open and closed symbols. Numbers to the right of each graph are calibrated radiocarbon ages (Colman et al., this volume).

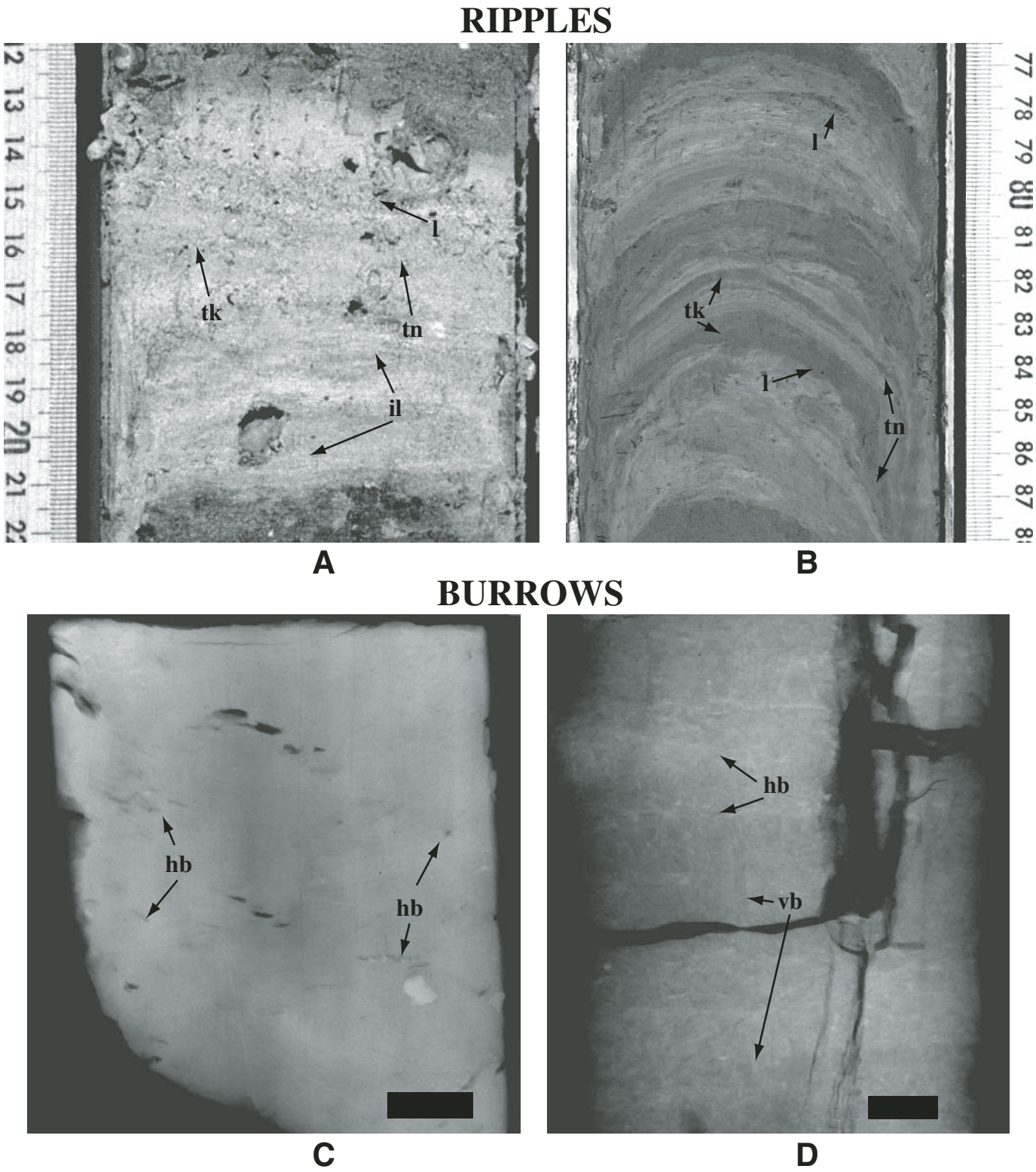

Figure 8. Depth-sensitive sedimentary structures. (A) Medium to fine sand with wave-ripple structures at site BL02-1. Ripples are recognized as lenses (l) and layers that thicken (tk) and thin (tn) laterally. Some ripples show internal lamination (il) that indicates vortex ripple forms. Aragonite mud interbeds are lighter colored. Scale is in centimeters. (B) Wave-ripple structures in siliciclastic sediment of core BL2K-2-1. Fine to medium sand forming lenses (l) and laminae that thicken (tk) and thin (tn) laterally represent rolling-grain ripples. Scale is in centimeters. (C) Aragonite mud with small horizontal burrows (hb) viewed in an X-ray image from core BL96-1. The limited size and horizontal orientation suggest low oxygen availability with limited infauna. Scale bar is 1 cm. (D) Siliciclastic mud with abundant randomly oriented burrows including vertical (vb) and horizontal (hb) orientations viewed in an X-ray image from core BL96-3. The variable sizes and orientations suggest a well-oxygenated environment with varied infauna. Scale bar is 1 cm.

properties (Clifton, 1976; Harms et al., 1982). For instance, rolling-grain ripples form at the initiation of sediment movement under wave bottom-shear stress, whereas vortex ripples require higher shear stress under the same depth and grain-size conditions. Rolling-grain ripples have broad crests and large wavelength-to-height ratios in contrast to vortex ripples, which have sharper crests and smaller wavelength-to-height ratios. In cross section, rolling-grain ripples appear as thin, elongate lenses with no internal stratification, whereas vortex ripples comprise thicker, shorter lenses with internal cross-lamination (i.e., Harms et al., 1982). Smoot and Benson (1998) extended this concept to include wave-formed lag deposits, and noted that the relative abundance of locally derived shell material incorporated in wave-formed deposits increases with distance from external source areas such as mountain fronts or river mouths. The Bear Lake sediment cores provide only a few opportunities to use wave-formed ripple types as depth constraints. Wave-formed deposits in cores taken many kilometers from the modern shoreline clearly show the impact of distance from external source areas by the predominance of shell material over clastic grains. These deposits appear to be less apparent in grain-size analyses of siliciclastic residue.

As discussed in the section on grain size, sediment focusing occurs frequently regardless of lake size. Basin geometry controls the amount of sediment transported lakeward with steeper basin floors promoting more transport (Hakanson, 1977, 1982; Blais and Kalff, 1995). Falling lake levels change the dynamics of this relationship by exposing more fine-grained sediment initially deposited in deep water to wave conditions, shifting the location of proximal wave-formed turbidites basinward, and decreasing the surface area for distribution of wave-reworked sediment (Smoot and Benson, 2004). In contrast, rising lake levels engender the reverse of these conditions. The net effect is that the sedimentary record of sediment focusing is more pronounced in falling lakes than in rising lakes. In Bear Lake sediment cores, zones with pronounced evidence of sediment focusing are interpreted as indicative of falling lake levels. The intervals of increased sediment focusing are recognized by smear-slide analysis, and by distinct intervals with more scattered coarse grains or graded intervals with sharp, erosional bases (Smoot, this volume). The latter are interpreted as wave-formed turbidite deposits that increase in size and frequency with falling lake levels.

A variety of burrowing styles occur in Bear Lake sediment (Smoot, this volume). The nature of burrows depends upon the type of organism, sediment type, the rate of sediment accumulation, water chemistry, and availability of food or oxygen (e.g., Hasiotis, 2002). Shifts in burrow style within a vertical sediment record indicate changes in one or more of these parameters. In Bear Lake, shifts from small, bedding-plane-parallel burrows to larger, more randomly oriented burrows (Figs. 8C and 8D) may indicate changes in water depth. Smoot and Benson (1998) argued that the degree of lake stratification controls available oxygen on the lake floor, which changes the assemblage and strategies of burrowing organisms. When the water column is well stratified, low-oxygen bottom conditions limit burrowing to a small fauna that mine only the upper sediment surface. In contrast, when the water column is well mixed, well-oxygenated bottom conditions allow a richer fauna with more vertical mixing of sediment. Chemical stratification is more likely to occur during rising lake levels when freshwater inflow overlies more concentrated water from the lowstand. At Bear Lake, small bedding-plane-parallel burrows are associated with core intervals with little evidence of sediment focusing, whereas large random burrows are associated with intervals that are dominated by features indicating sediment focusing. This strengthens the interpretation that the amount and type of burrowing reflect changes in lake level.

The presence of vertical root structures requires either subaerial exposure or very shallow water. Subaqueous plants produce tiny "holdfast" roots, which are restricted to the upper 1–2 cm of sediment (Hutchinson, 1975). Vertical roots that are 1 mm in diameter or larger probably represent subaerial vegetation. Root casts in the Bear Lake cores are distinguished from burrows by tapering diameters, bifurcation into smaller diameters, and carbonaceous residues (Fig. 9). The distinction between root structures and burrows is not always straightforward, particularly with large sediment-filled root casts. In the Bear Lake cores, root structures are commonly associated with other soil-like features such as cutans, carbonate concretions, and evaporites (Smoot, this volume). Root structures penetrate the sediment, so they may occur within subaqueous deposits, reflecting later subaerial exposure.

The use of sedimentary textures as lake-level indicators has both strengths and weaknesses. Sedimentary textures are measured continuously, are independent of vertical scale, and use multiple criteria to identify even small changes in depositional environment. The variability of sediment characteristics, however, also makes the categorization of sediment packets more subjective than the straightforward physical measurements of grain size or color. Thus, a subtle indicator of a lake-level change may be lost in the sediment categorization. In addition, the distributions of modern sedimentary textures are poorly constrained because the uppermost water-rich deposits were not preserved as undisturbed core. Furthermore, some of the sedimentary textures do not have modern analogs. Therefore, sedimentary textures provide a high probability for recognizing relative lake-level changes, but low precision for quantifying absolute lake-level changes.

Sedimentary Texture Results

Bear Lake sediments can be broadly divided into several sediment categories: aragonite mud, calcite mud, shell-rich sand and gravel, mixed calcitic-siliciclastic mud, and siliciclastic mud (Fig. 10; Smoot, this volume). These sediments define a basic stratigraphy. Upper and lower aragonite zones are separated by a calcite zone that is easily correlated among the cores. A second calcite zone underlies the lower aragonite and overlies a mixed calcitic-siliciclastic mud interval. A third calcite zone underlies this mixed interval and overlies a zone of siliciclastic sediment that extends to the base of the studied section.

The upper and lower aragonite zones are subdivided into three types, which are distinguished by sedimentary textures, predominately grain-size distribution and diatom characteristics (Smoot, this volume). Aragonite I, which has an intermediate grain size, is the dominant type found in the upper part of deep-water cores (i.e., BL 96-1, BL96-2, BL02-3, and BL02-4), whereas the coarser-grained Aragonite III is more common in the upper parts of shallow-water cores (BL02-1, BL02-2, BL2K-2, BL02-5, and BL96-3). Aragonite II is finer grained than the other two types, contains small pelagic diatoms (Moser and Kimball, this volume), and is restricted to the two deepest-water cores (BL96-1 and BL96-2). Aragonite II was not identified in BL02-3, which was taken at the same depth as BL96-2 (43 m), suggesting either that they were taken at the shallowest depth boundary for Aragonite II or that some factor other than depth controls the distribution of the fabric. The distribution of the different types of aragonite mud and their relative grain sizes are interpreted as indicating relative lake depths. Aragonite III is the shallowest-water type and Aragonite II as the deepest-water type. In contrast to the quantitative grain-size data discussed previously, the grain sizes discussed here include shelly material, crystals and grains of carbonate, as well as siliciclastic material. Changes in grain size of siliciclastic material roughly coincide with boundaries between Aragonite I and Aragonite III, but do not distinguish between Aragonite I and Aragonite II.

Calcite mud, which has virtually no aragonite or clastic sediment in smear slides, is interpreted as occurring in a rising lake or deep lake. The calcite intervals, which, in part, also include mixed carbonate and siliciclastic components, are believed to represent the highest Holocene lake levels because they are continuous across a range of water depths with little change in character, they are very fine grained, and they have a predominance of small pelagic diatoms (Moser and Kimball, this volume).

Sediment composed of shell-rich sand and gravel indicates shallow water or shoreline deposits. These deposits commonly overlie erosional surfaces.

Sediment composed of mixed calcite and siliciclastic material occurs in two settings. In the Holocene record, such deposits

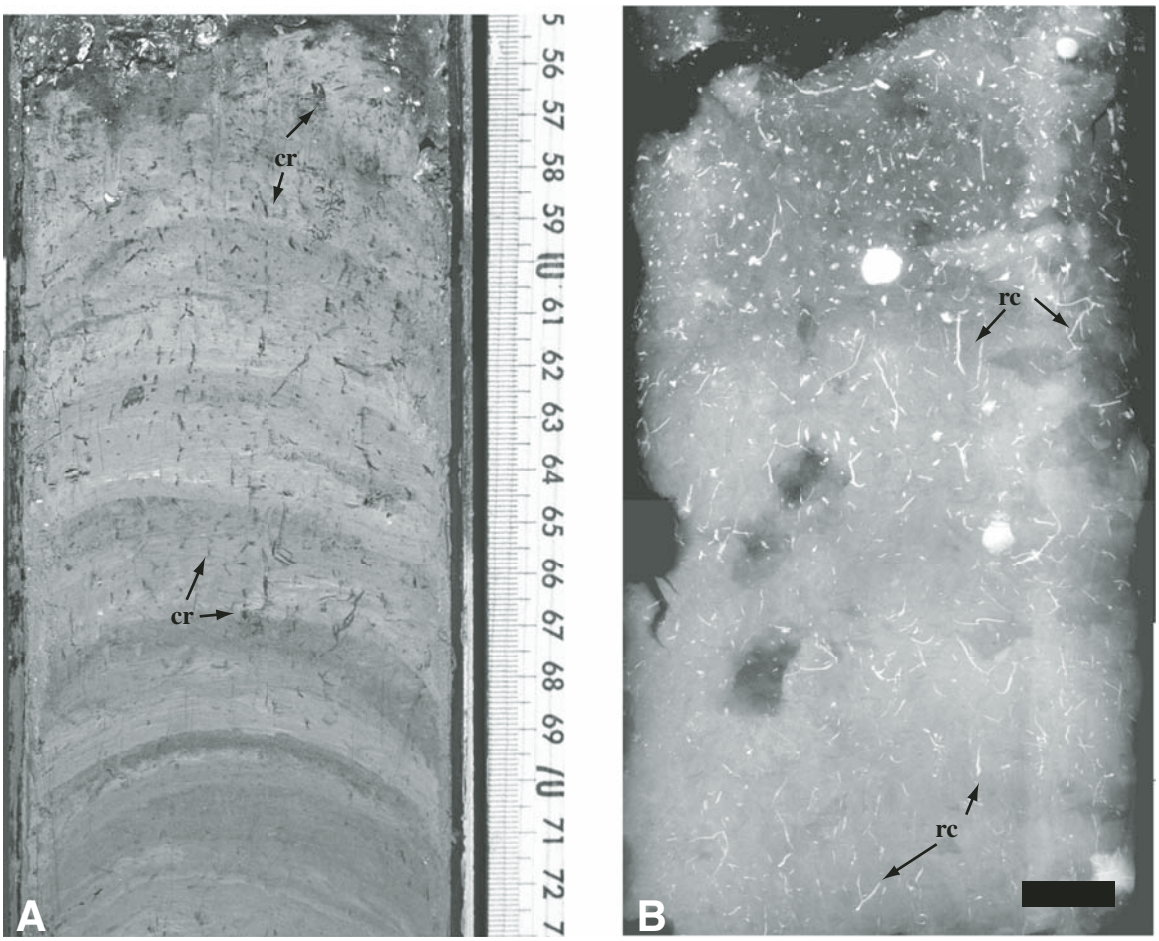

Figure 9. Root-like structures in cores. (A) Carbonized root-like structures (cr) with pyrite coatings in core BL2K-1. Note how the features decrease in size and abundance downward. Scale is in centimeters. (B) Root-like casts lined with framboidal pyrite (rc) viewed in an X-ray image of a section of BL96-3. Note how features decrease in size and abundance downward. Large white circular features are carbonate concretions interpreted as soil features. Scale bar is 1 cm.

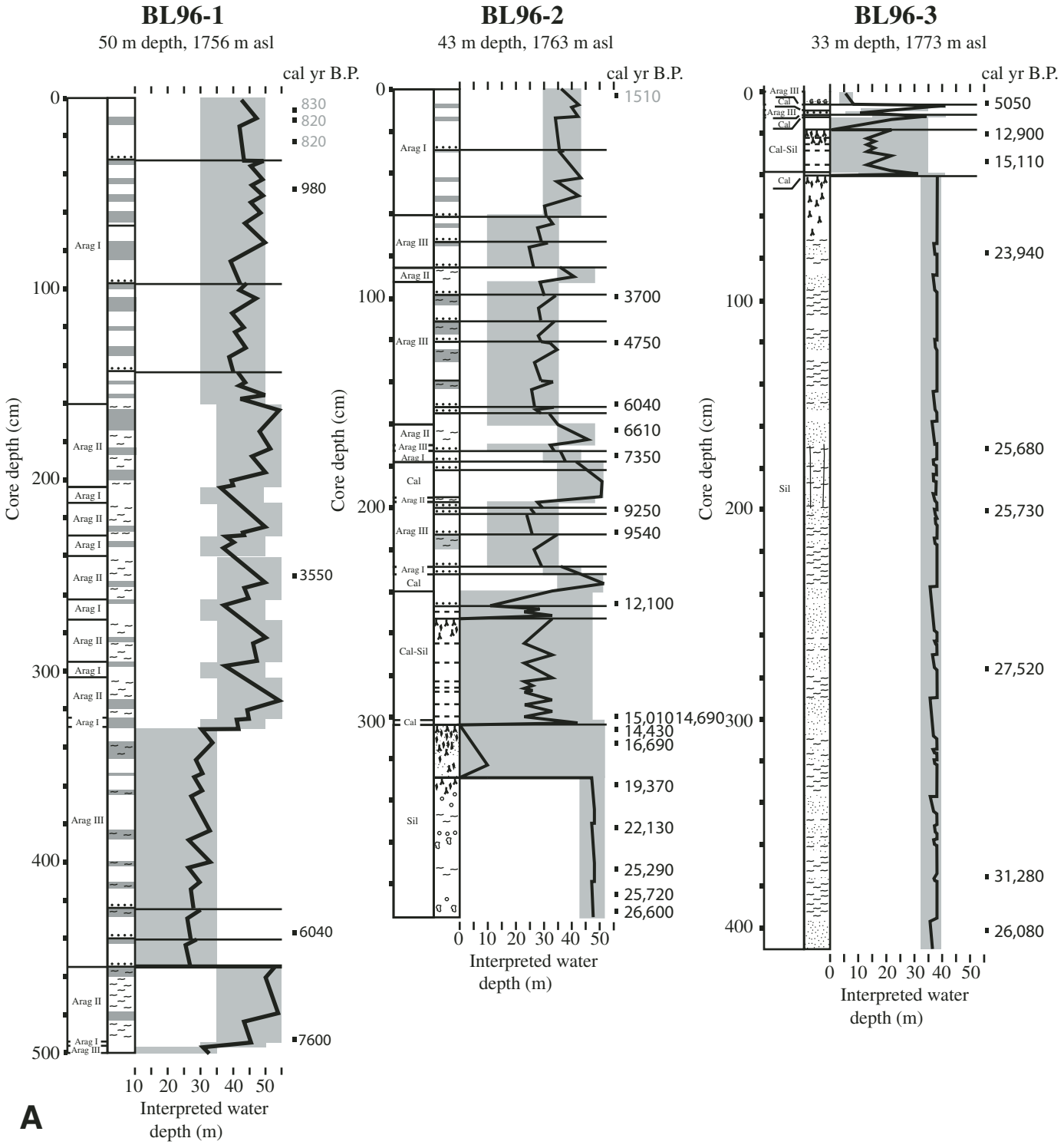

Figure 10 (*continued on next page*). Depth models based on sedimentary textures in cores BL96-1, BL96-2, and BL96-3 (A) and at core sites BL02-3 and BL02-4 (B). Each core shows the sediment type as defined by Smoot (this volume) and the significant sedimentary structures. Interpreted depths are shown by the black lines, with gray areas signifying the range of possible depths based on this technique. Black horizontal lines indicate sharp bedding surfaces (with coarser-grained sediment overlying finer-grained material) that may indicate erosion. Numbers to right of column are calibrated radiocarbon dates (Colman et al., this volume). Scale to left of each core is in centimeters. Legend appears on following page. In Figure 10B, photographs of core segments are left of the schematic drawings, and curves composed of dashed lines represent modeled depths from grain-size data (Fig. 7). asl—above sea level.

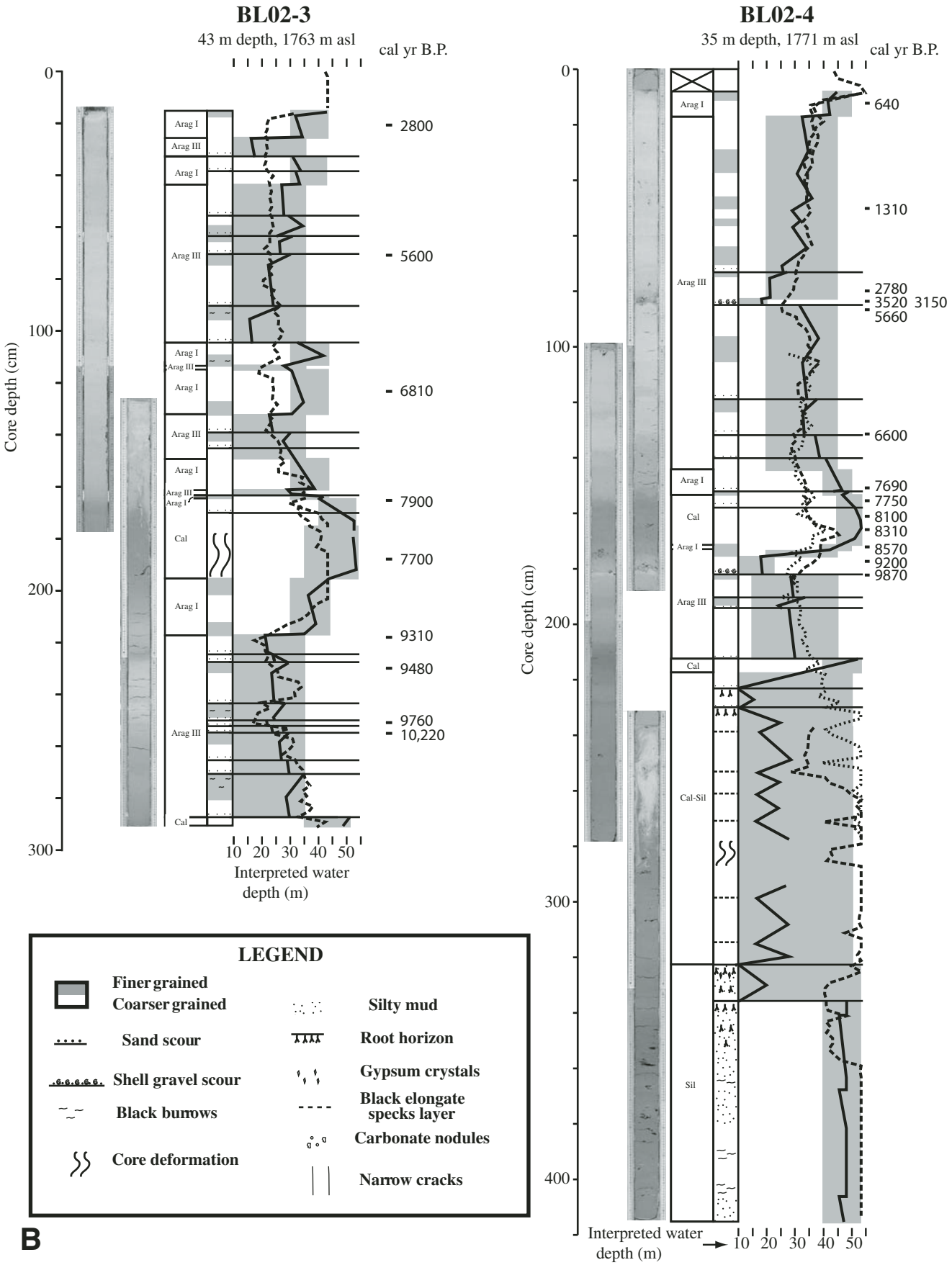

Figure 10 (*continued*).

reflect marsh sedimentation north of the lake (Smoot, this volume). Deposits with similar root features, organic-rich bands, and tiny gastropods occur in core BL02-1 (100–170 cm depth). In the Pleistocene section, mixed calcite and siliciclastic mud deposits comprise an interval between the aragonite deposits and the underlying siliciclastic mud. The water-depth interpretations for these deposits are uncertain, because they have no modern analog. Their association with horizons of root casts suggests they were formed in shallow water, but their fine grain size is more consistent with deposition in deep water.

Siliciclastic mud intervals were deposited when the Bear River was a major source of sediment and Bear Lake was spilling (Dean et al., 2006; Kaufman et al., this volume). Siliciclastic mud in the shallow part of the lake (cores BL2K-2, BL02-1, and BL02-2) is sandier than correlative sediment from the deeper parts of the lake, suggesting a depth not much greater than the modern lake. Wave-formed ripples in BL2K-2 constrain the depth at least intermittently to less than 5 m above the modern lake. This interpretation is consistent with the dearth of shoreline features in the same age range (discussed earlier) as the siliciclastic mud intervals in the cores.

In addition to this broad division of sediment types, there are other indications of lake-level fluctuation. These indications largely reflect differences in sediment focusing and occur in each type of aragonite mud. The variability is most pronounced in Aragonite I, whereas in Aragonite III, greater sediment focusing is characterized by more abundant rock fragments and broken diatoms. In Aragonite II intervals, greater sediment focusing is indicated by small-scale transitions into Aragonite I. Sediment focusing is also indicated in the upper portions of calcite mud intervals. Intervals that display more sediment focusing are interpreted as deposits from shallower water than intervals of the same mud type that lack evidence of sediment focusing. This interpretation is supported by shifts in bioturbation patterns. Small bedding-plane-parallel burrows are typical of the finer-grained intervals interpreted as rising lake levels, and random burrows are associated with increased sediment focusing. The magnitude of lake-level change represented by these variations is not well established, but, by comparison to modern lake fluctuations (Dean et al., this volume), is thought to be on the scale of ~5 m in most cases.

Horizons from which root-cast sequences extend downward are found in BL96-2, BL96-3, BL02-3, BL02-4, BL02-5, BL02-2, BL02-1, and BL2K-2 (Smoot, this volume). These horizons are interpreted to have formed when lake level regressed below the core site. There are at least three such horizons in core BL96-2, each indicating that lake level was below 1763 m asl. Rooted horizons occur in similar stratigraphic positions in the other cores, and a fourth rooted horizon in BL02-4 occurs in a position equivalent to a sandy layer in BL96-2 (Smoot, this volume). Two of the root-cast sequences are within the siliciclastic mud interval, including its upper boundary, and two of them are within the mixed calcitic-siliciclastic mud interval. As mentioned earlier, the bulk of the siliciclastic mud interval was probably deposited at depths at or slightly greater than that of the modern lake. The two rooted horizons are interpreted as indicating a rapid drop in lake level, with a slight transgression within the lowstand.

Water-depth indicators associated with the mixed calcitic-siliciclastic mud are equivocal. Horizons that contain small horizontally elongated sulfide coatings that appear to be tubes may represent development of subaqueous vegetation, but the features could also be burrows or some other tube-shaped feature. Subaqueous vegetation would be consistent with shallow water (around 10–20 m maximum depth). The mixed calcitic-siliciclastic mud interval thins from 60 cm in BL96-2 to ~25 cm in BL96-3 (1773 m asl), and is missing in BL02-5 (1783 m asl) and shallower cores. BL02-1 (1796 m asl) contains a marsh deposit (100–170 cm depth) that is at least partly correlative to the mixed calcitic-siliciclastic mud interval, suggesting two possible depth scenarios for the lake (Fig. 11). Nearly pure calcite mud intervals occur at the base and top of the mixed calcitic-siliciclastic mud interval. These suggest deep-water conditions, so the associated root-cast horizons may have formed during lowstands and may have no bearing on depth at the time of deposition.

LAKE-DEPTH MODELS

Sedimentary textures and shorelines were used to construct models of lake depth changes (Fig. 10). For these models, sediment types constrain the probable range of depths. The maximum depth of Aragonite I is 50 m, the depth of core BL96-1, and the minimum depth is 35 m, the depth of BL02-4. Aragonite II represents lake depth greater than 50 m. The maximum depth of Aragonite III is taken as 33 m, the depth of BL96-3, and the minimum depth is 18 m, the depth of BL02-2. The assemblage of sedimentary features in calcitic mud and their continuity even in cores from modern shallow-water environments suggest they represent the greatest depths. Sediments of the Willis Ranch and Raspberry Square highstands are the highest features (1814 m asl) within the age range of these deposits. Lake elevation during deposition of much of the siliciclastic mud is assumed to be near the elevation of the Lifton shoreline (1808 m asl) given the constraints for forming wave vortex ripples in fine sand in cores BL2K-2 (1797 m asl), BL02-1 (1796 m asl), and BL02-2 (1787 m asl), and the absence of shorelines of similar age above or below the Lifton shoreline. Two additional assumptions provide further constraints on the model. First, within a given sediment type, coarser grains and erosional surfaces indicate shallower water. For instance, an increase in evidence of sediment focusing is modeled by a 5 m decrease in water depth. Second, within the calcitic-siliciclastic mud, small horizontal tubes are taken to indicate shallower water than sediment lacking such tubes. These assumptions are reasonable, but the upper-limit assumptions for all but the calcite mud are largely unsubstantiated.

Comparison of results for the upper aragonite mud interval among the different cores shows some variability in the interpreted lake-depth histories (Fig. 10). Modeled depths for core BL96-1 are consistently greater in the upper 330 cm and lowest 45 cm than in the intervening 115 cm, where modeled depths fluctuate

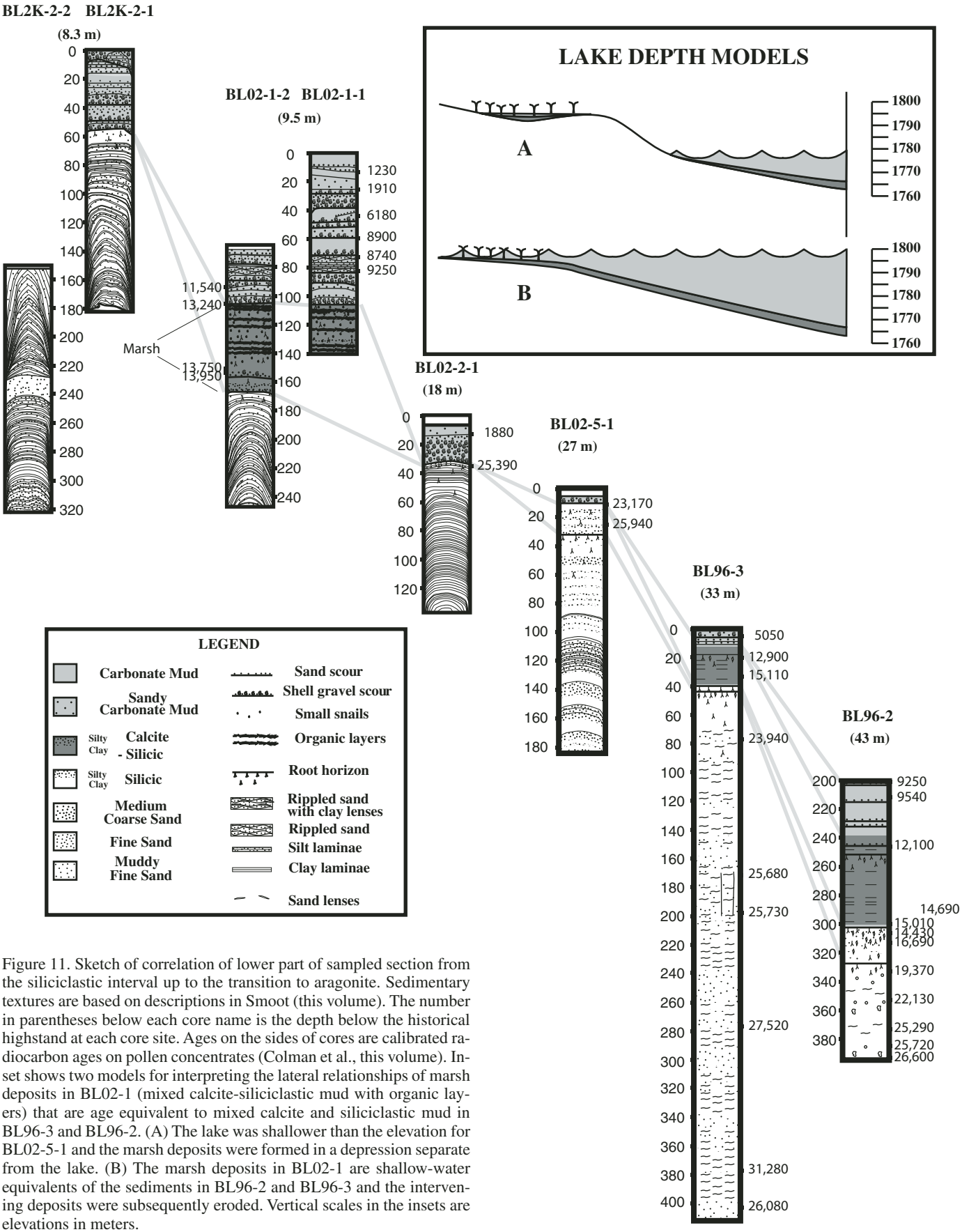

Figure 11. Sketch of correlation of lower part of sampled section from the siliciclastic interval up to the transition to aragonite. Sedimentary textures are based on descriptions in Smoot (this volume). The number in parentheses below each core name is the depth below the historical highstand at each core site. Ages on the sides of cores are calibrated radiocarbon ages on pollen concentrates (Colman et al., this volume). Inset shows two models for interpreting the lateral relationships of marsh deposits in BL02-1 (mixed calcite-siliciclastic mud with organic layers) that are age equivalent to mixed calcite and siliciclastic mud in BL96-3 and BL96-2. (A) The lake was shallower than the elevation for BL02-5-1 and the marsh deposits were formed in a depression separate from the lake. (B) The marsh deposits in BL02-1 are shallow-water equivalents of the sediments in BL96-2 and BL96-3 and the intervening deposits were subsequently eroded. Vertical scales in the insets are elevations in meters.

around ~25 m bml. The uppermost 160 cm varies between the modern level and ~10 m bml, whereas the interval from 160 to 330 cm shows greater fluctuations, varying from ~15 m bml to ~3 m above modern level. Modeled depths for the upper 60 cm in BL96-2 fluctuate within 10 m of the modern level. Depths from the underlying 100 cm are mostly 10–20 m bml but rise to near modern lake levels in a 10 cm interval at a core depth of 90 cm. Underlying this lowstand sequence is a 15 cm highstand sequence that contains a sharp peak that rises above the modern level. In the upper 40 cm of BL02-3, modeled depths indicate two periods when lake levels were ~10 m bml, separated by a period when the lake was 15 m lower. Modeled depths from the underlying 65 cm are mostly ~10–15 m bml beginning following a lowstand ~25 m bml at a core depth of 95–105 cm. Underlying this lowstand sequence is a highly fluctuating sequence from 105 to 160 cm that includes two peaks to near modern lake level and a lowstand interval at ~20 m bml. Near the base of the upper aragonite zone, modeled lake-level falls from above the modern level in the calcite zone to ~15 m bml. In the upper 15 cm of BL02-4, modeled depths are within 5 m of the modern lake. Modeled depths in the underlying 120-cm-thick interval are mostly between 10 and 15 m bml, with an interval ~25 m bml at ~85 cm. Within the interval 135–170 cm (overlying the calcite mud), modeled depths range from greater than modern depths to 10 m bml. The abbreviated section in BL96-3 indicates depths ~25 m bml.

Interpreted histories for the lower aragonite zone also show core-to-core variations. For BL96-2, modeled depths are mostly 15 m bml and indicate one peak within 5 m of the modern level. For BL02-3, modeled depths show a peak within 5 m of modern before falling ~15 m then rising gradually to the contact with the overlying calcite zone. In BL02-4, the lower aragonite interval is only 35 cm thick. The modeled depth history indicates mostly lake levels ~15 m bml with one minimum 10 m lower followed by an abrupt rise to the overlying calcite zone. In BL96-3, the 2-cm-thick aragonite mud interval indicates lake levels ~20 m bml.

The mixed calcitic-siliciclastic mud interval varies in thickness among the three cores (Fig. 10). Seven horizons with small horizontal tubes occur below the root-cast horizon in BL96-2. Six such horizons occur below the lower root-cast horizon in BL02-4, and four occur below the root-cast horizon in BL96-3. It is difficult to compare this interval in cores BL96-2 and BL02-4 because sedimentary structures in this part of BL02-4 are not as well defined as in the other cores. X-radiography was not used to study BL02-4 (Smoot, this volume) and the top of the deepest core segment from this site was highly disturbed (Fig. 10B). The three closely spaced horizontal tube horizons in BL96-3 and BL96-2 may be correlative. If so, a large part of the BL96-3 mixed calcitic-siliciclastic mud interval below the root-cast horizon was eroded.

The siliciclastic mud interval is characterized by a pattern of upward-coarsening sequences at each site where it was sampled (BL96-2, BL96-3, and BL02-4). Two complete sequences were penetrated in both BL96-2 and BL02-4. In BL96-3, the sequences are much more layered and coarser grained. The upward-coarsening successions vary from ~40-cm to ~80-cm thick, and there is a suggestion of a larger-scale upward coarsening sequence ~130-cm thick. The sequences are shown as shallowing successions, but they may have more to do with shifts in abundance of source material (Rosenbaum and Heil, this volume) or changes in the inflow (Smoot, this volume). The siliciclastic mud interval has two root-cast sequences in the uppermost few decimeters including the contact with the mixed calcitic-siliciclastic mud. These indicate that lake levels fell at least 43 m below the modern lake level. In BL96-2 and BL96-3, the immediately overlying material is a calcite mud that is interpreted as a transgressive deposit. The absence of this calcite mud in BL02-4 suggests that it may not indicate conditions as deep as the younger calcite layers, although it is possible that the layer was missed in BL02-4.

Comparison of Depth Models from Grain-Size Data and from Textural Features

Modeled lake levels determined from grain-size data and independently from sedimentary textures can be directly compared for cores BL02-3 and BL02-4 (Fig. 10B). The grain-size model for the aragonite and calcite mud intervals generally indicates shallower-lake conditions than the sedimentary-texture model, but well within the ranges of possible depths for each sedimentary texture. The two methods generally produce the same sense of change, but the magnitude of change is frequently different. The onset of changes is also slightly different in many places.

Several factors contribute to the differences produced by the two techniques. The textural features include chemical and biogenic sediments that are excluded from the grain-size data. Aragonite III is distinguished from Aragonite I by the abundance of broken and abraded diatoms and ostracodes in the former. The small portions of siliciclastic material in the aragonites may not have enough variability to distinguish between these fabrics. Sandy beds overlying sharp and sometimes irregular contacts are not always recognized in grain-size data because samples either missed these beds or averaged coarse-grained material with adjacent fine-grained sediment. Burrow mixing of sediment between layers may also contribute to smoothing of the grain-size data. For instance, thin, very-fine-grained carbonate layers are not apparent in the grain-size data because of burrow mixing across boundaries. The assessment of near modern lake conditions for Aragonite I, however, is not verifiable due to a lack of surface sediment for comparison, and the grain-size data indicate that this may not be a good assumption. If lower lake levels were assumed for this fabric, the texture-based model would indicate levels more akin to the grain-size model.

The grain-size model for calcitic-siliciclastic mud in BL02-4 suggests depths at the model maximum for most of the thickness and minor intervals with drops to modern depths or 5 m below modern depths. The textural evidence for shallow lake conditions in the mixed calcitic-siliciclastic mud intervals is equivocal. If the lake was shallow, the absence of wave features is difficult to explain. If the tiny horizontal tube features are correctly interpreted as root hairs, perhaps they formed under tens of meters

of clear water. Marsh deposits in BL02-1 (Fig. 11) provide the strongest constraint on lake depth during deposition of the mixed calcitic-siliciclastic mud interval, thus establishing that as the maximum lake elevation (1796 m asl) for that interval. The conflicting values with the grain-size model are attributed to the effect of siliciclastic sediment input, which is not present in the modern depth model. The minor coarser-grained intervals within the calcitic-siliciclastic mud appear to be coincident with the presence of sulfide-coated egg casings and carapaces (Smoot, this volume) that may have skewed the results.

As noted earlier, the grain-size model is not applicable to the siliciclastic mud interval. The best lake-level constraints for the siliciclastic mud interval are the absence of beach deposits of similar age and the presence of marsh and fluvial deposits of similar age in the area north of the lake at elevations lower than the Lifton shoreline deposits. Increases of the silt content of BL96-2 and BL96-3 are interpreted as indicators of shallower lake depths, which are correlative to shifts from predominately silt and clay to sand-rich intervals in cores from sites BL2K-2, BL02-1, and BL02-2.

CHRONOLOGY

In order to combine the records from the various cores into a single lake-depth history, chronologies for the different data sets must be consistent. Most of the radiocarbon ages for the cores are from pollen concentrates (Colman et al., this volume). A few ages were obtained from ostracode shells, total organic carbon, and mollusk shells. The pollen concentrates contain small amounts of other carbon-bearing material that may be detrital in character. Colman et al. (this volume) interpret a reservoir effect (Broecker and Walton, 1959; Olsson, 1986; Bjorck and Wohlfarth, 2001) of 370 years for the ostracode ages by comparing ages of ostracodes and pollen from the same horizons. A similar comparison between pollen and total organic carbon ages suggests that ages from total organic carbon are too old by ~480 years. There has been no attempt to establish a reservoir effect on the shells of snails or clams, although ages of shell layers and pollen-derived ages from adjacent layers suggest that a reservoir effect of ~400 years is reasonable. There are no data available to determine if the reservoir effect varied with lake depth or species.

Smoothed Age Models

Colman et al. (this volume) developed age models for cores BL96-1, BL96-2, BL96-3, BL02-3, and BL02-4 using both polynomial and cubic spline techniques. With the exception of core BL02-4, each core was assumed to be continuous with no significant breaks or abrupt variations in sedimentation rate. The age model for core BL02-4 consisted of three curves separated by age breaks at shell gravel layers thought to indicate unconformities. Within the siliciclastic mud interval that Rosenbaum and Heil (this volume) interpreted as dominated by glacial flour, Colman et al. (this volume) rejected five radiocarbon ages (from pollen concentrates) from each of cores BL96-2 and BL96-3. They noted that pollen within this interval is sparse and poorly preserved in contrast to the underlying and overlying strata. Their age models for BL96-2, BL96-3, and BL02-4 through the siliciclastic interval are based on ages above the interval dominated by glacial flour, a calibrated age of 26,080 yr B.P. from the bottom of BL96-3 (just below the interval dominated by glacial four), two radiocarbon ages from BL00-1 (below the interval dominated by glacial flour) that are consistent with the age from the base of BL96-3, and correlation of horizons among the cores. The two curve-fitting techniques discussed by Colman et al. (this volume) yield nearly identical results within the limits of error, and correlations among cores based on geochemistry and magnetic properties are consistent with these age models.

The initial step in construction of a combined lake-level curve is to convert lake depths to surface elevations. This was accomplished by assuming that the elevation of each core site was constant through the time of sediment accumulation. There was no attempt to correct for variations in accumulation rate versus subsidence. Comparison of interpreted lake-elevation curves for individual cores (BL96-1, BL96-2, BL96-3, BL02-3, and BL02-4) shows some scatter at any time. General trends of rising and falling lake level are more or less synchronous. However, taking the age models at face value, there are significant intervals with conflicting senses of lake-level change (examples shown in Figs. 12A and 13A). Such conflicts occur ca. 1000, 2500, 3400, 3800, 4300, 5200, 5700, 6900, 9000, 9500, 10,000, 10,500, 10,900, 11,300, and 11,700 cal yr B.P. The models also indicate that a root-forming event at 1763 m asl coincides with a lake at 1806 m asl (ca. 18,300 cal yr B.P.), whereas a root-forming event at 1773 m asl coincided with lake level at 1810 m asl (ca. 23,700 cal yr B.P.). Lake-level variations must be synchronous at each location. Therefore, if the sedimentary evidence is interpreted correctly, the smoothed age models have incorrectly presented the rates of deposition in at least some of the cores.

Alternative Chronology

Sedimentological evidence of erosional surfaces overlain by coarse sediment indicative of breaks in sedimentation (like those in the age model for core BL02-4) occurs in all of the cores, but commonly with more subtle textural expressions. The variety of textural styles recognized in the cores also suggests that sedimentation rates may be highly variable. Therefore, an alternative approach to chronology is required. In this approach, the emphasis is on observable differences in the sediment and the correlation of depositional conditions rather than on mathematical simplicity.

The alternative approach employs an iterative procedure (Fig. 14). The core from the greatest depth (BL96-1) was plotted first. Ages were linearly interpolated between dated horizons and extrapolated to the core ends (Fig. 14A). The second deepest-water core (BL96-2) was then placed on the same plot with the radiocarbon dates constraining the ages (Fig. 14B). Using the same depth proxies, the intervals between constraining radiocarbon

ages on both cores were adjusted so that the sense of lake-level change is synchronous (Fig. 14C). If possible, the relative magnitudes of lake-level change were also aligned. Erosional surfaces were then aligned, so that each erosional surface in the deeper-water core is equivalent to a similar surface in the shallower-water core. If insertion of an erosional gap allowed a better alignment of the records, the gap was constrained by the following requirements: that erosion was greater in the shallower core, that the erosion began earlier in the shallower core, and that sedimentation resumed earlier in the deeper-water core. This procedure was repeated for all well-dated cores with overlapping records (Fig. 14D), and for dated portions of cores lacking extensive age control. Where present, grain-size-based depth curves were adjusted in the same manner as curves based on sedimentary features from the same core. Shoreline data were placed on the same plot. The subaerial shorelines appear to be completely out of phase with any of the depth indicators in the core. A reasonable argument—assuming the shoreline data are the most reliable—would be to discard all core data. As previously discussed, however, subaerial shoreline data have poor age control due to the reliance on ages from shells, but are the best indicators of true depth. Therefore, shoreline deposits were used to constrain lake depth for relatively broad time intervals. For instance, the Willis Ranch and Raspberry Square highstand deposits are the highest features with age ranges that overlap the cored intervals. The calcite layers in the cores have the grain-size range, textural characteristics, and distribution that indicate the deepest-water conditions. If the two most continuous calcite layers are correlated with the two highest shorelines, the other shoreline depth constraints fall roughly in phase with the core data. Although this approach requires an assumption that the shoreline ages are too old, the difference is consistent with observed problems in the cores and reasonable processes in the shoreline environment.

Most of the variability in the composite lake-level history (Figs. 12B and 13B) results from differences between depth estimates based on grain-size data and those based on sedimentary features. In some cases, relative lake-level changes could not be reconciled with the radiocarbon ages. In these situations, one of the ages must be assumed to be incorrect, if the assumptions about synchronous lake-level rise and fall are valid.

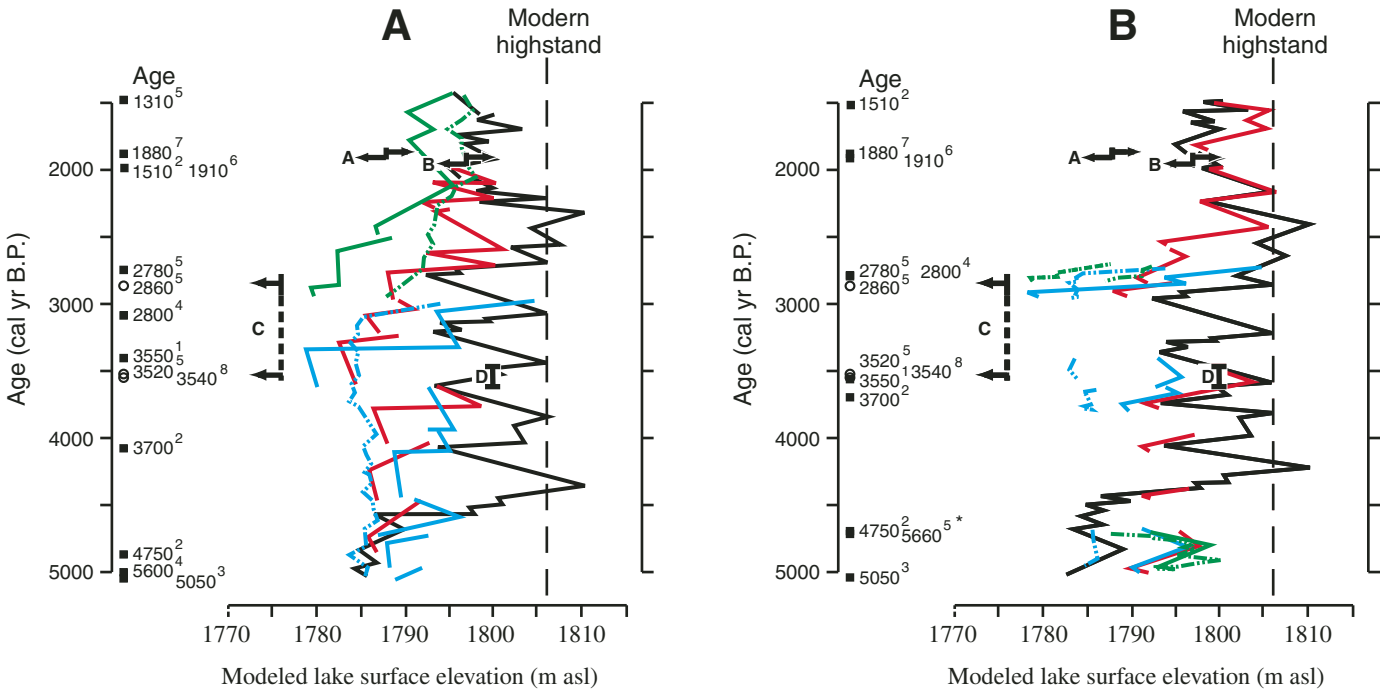

Figure 12. For the period 5000–1500 cal yr B.P., interpretations of lake-surface elevation history for individual cores and different types of data using (A) the smoothed age model of Colman et al. (this volume) and (B) the alternative chronology described in the text. Lake-surface elevation curves utilize sedimentary texture models (solid lines) for cores BL96-1 (black), BL96-2 (red), BL02-3 (blue), and BL02-4 (green), and also grain-size models (dashed lines) for sites BL02-3 and BL02-4. The surface elevations at each core site were determined by adding modeled water depths to the elevation of the sediment surface at that site. Vertical bars indicate shoreline features listed in Table 1, and bars with arrows are depth-significant features from other cores. Arrows indicate the relative depth with respect to the core depth (shallower left and deeper right), and arrows in both directions indicate the relative transition in depth. The vertical lengths of bars indicate the analytical confidence of ages. A—Transition from gravel sheet to Aragonite III in BL02-2; B—Transition from gravel sheet to Aragonite III in BL02-1; C—Shell ages from gravel sheet in BL02-4; D—Shell age from gravel sheet in BL2K-3. Calibrated radiocarbon ages on pollen concentrates (filled boxes) and on shells (open circles) are from Colman et al. (this volume). Shell ages are reduced by 400 years. Superscripts for ages refer to cores: 1—BL96-1; 2—BL96-2; 3—BL96-3; 4—BL02-3; 5—BL02-4; 6—BL02-1; 7—BL02-2; 8—BL2K-3. Asterisk indicates age rejected in creating the alternative chronology. asl—above sea level.

Where possible, such conflicts were resolved by accepting the calibrated age that is most consistent with the greatest number of cores. When necessary, ages from sandy intervals were rejected because such intervals are likely to be contaminated by older material. We devised two age models using this technique, one that assumed the ages within the siliciclastic interval with poor pollen preservation are too old, and one using the same criteria for acceptance of ages as the rest of the core. The lake-level history for the deposits overlying the siliciclastic interval is unaffected by the two models. Only a few ages do not fall within their confidence intervals (Colman et al., this volume) on the composite age scale. Six ages were discarded for the following reasons: (1) An age of 640 cal yr B.P. in core BL02-4 is one of several out-of-order ages that are believed to be a result of sediment reworking following diversion of the Bear River into the lake ca. 1912. (2) Sediment characteristics of a sample yielding an age of 5660 cal yr B.P. in core BL02-4 are more consistent with deposits younger than 5600 cal yr B.P. in core BL02-3, and the sample may also contain reworked materials from the overlying sand. (3) The youngest age in BL96-1 (7600 cal yr B.P.) is in an interval that probably contains reworked material and the character of the deposits is inconsistent with material with similar ages in BL02-3 and BL02-4. (4) In BL02-3, an age of 7900 cal yr B.P. is plotted ~100 years younger than its confidence limits in order to maintain consistency with similar materials in BL02-4. The alternative is to assume that two ages within BL02-4 are incorrect. (5) An age of 7700 cal yr B.P. in BL02-3 is out of sequence and within fluidized sediment. (6) An age of 14,690 cal yr B.P. in BL96-2 is inconsistent with a second age of 15,010 cal yr B.P. in the same core and an identical age in BL96-3.

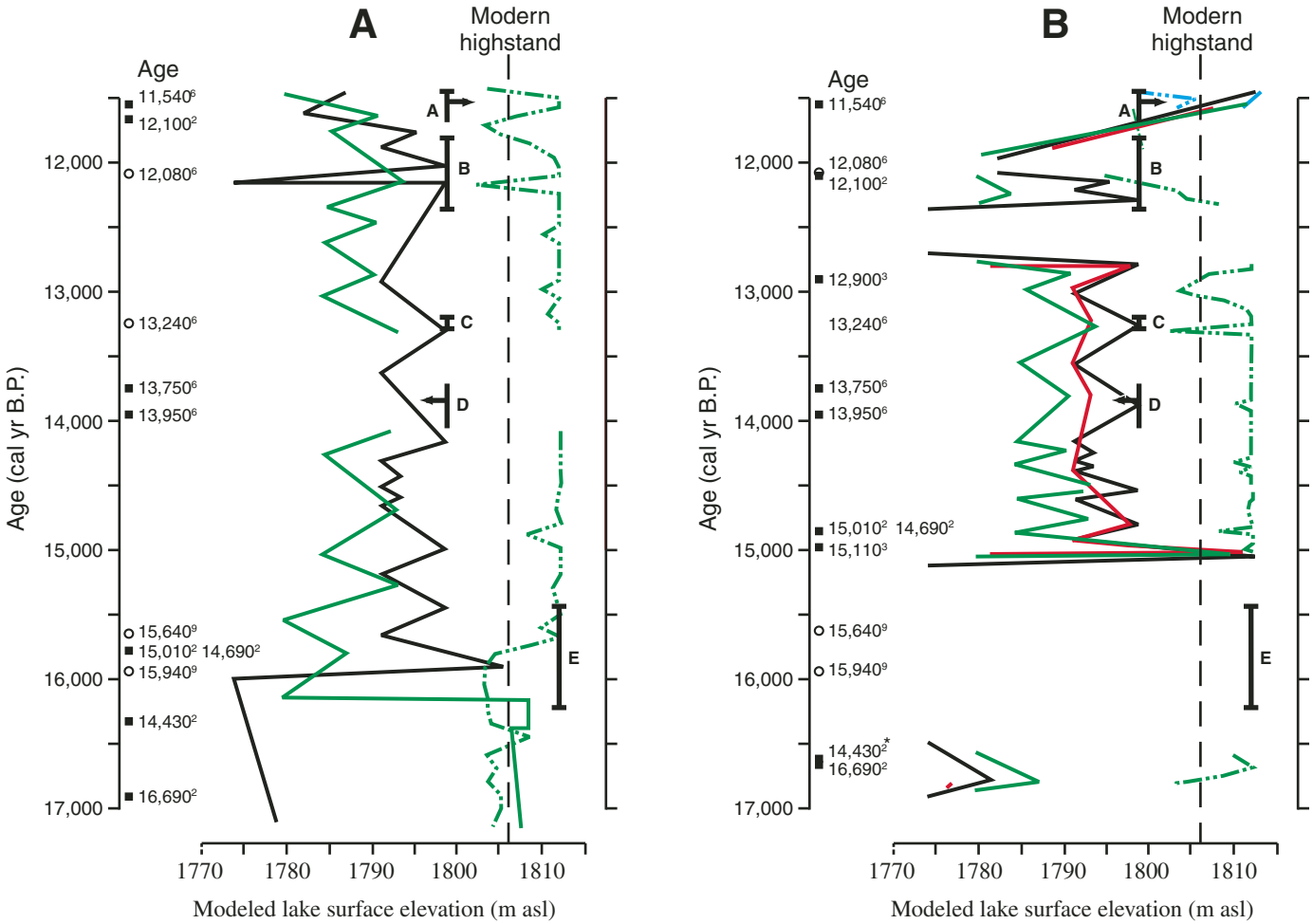

Figure 13. For the period 17,000–11,500 cal yr B.P., interpretations of lake-surface elevation history for individual cores and different types of data using (A) the smoothed age model of Colman et al. (this volume) and (B) the alternative chronology described in the text. Lake-surface elevation curves utilize sedimentary texture models (solid lines) for cores BL96-2 (black), BL96-3 (red), BL02-3 (blue), and BL02-4 (green), and also grain-size models (dashed lines) for sites BL02-3 and BL02-4. See caption for Figure 12 for explanation of numbers and symbols used in this figure. A—Aragonite overlying gravel sheet in BL02-1; B—Shell age from gravel sheet in BL02-1; C—Marsh deposit directly below gravel sheet in BL02-1; D—Marsh deposit in BL02-1; E—Shell ages from the deposits of the Raspberry Square phase. Ages with the superscript 9 from Laabs and Kaufman (2003). Shell ages are reduced by 400 years. asl—above sea level.

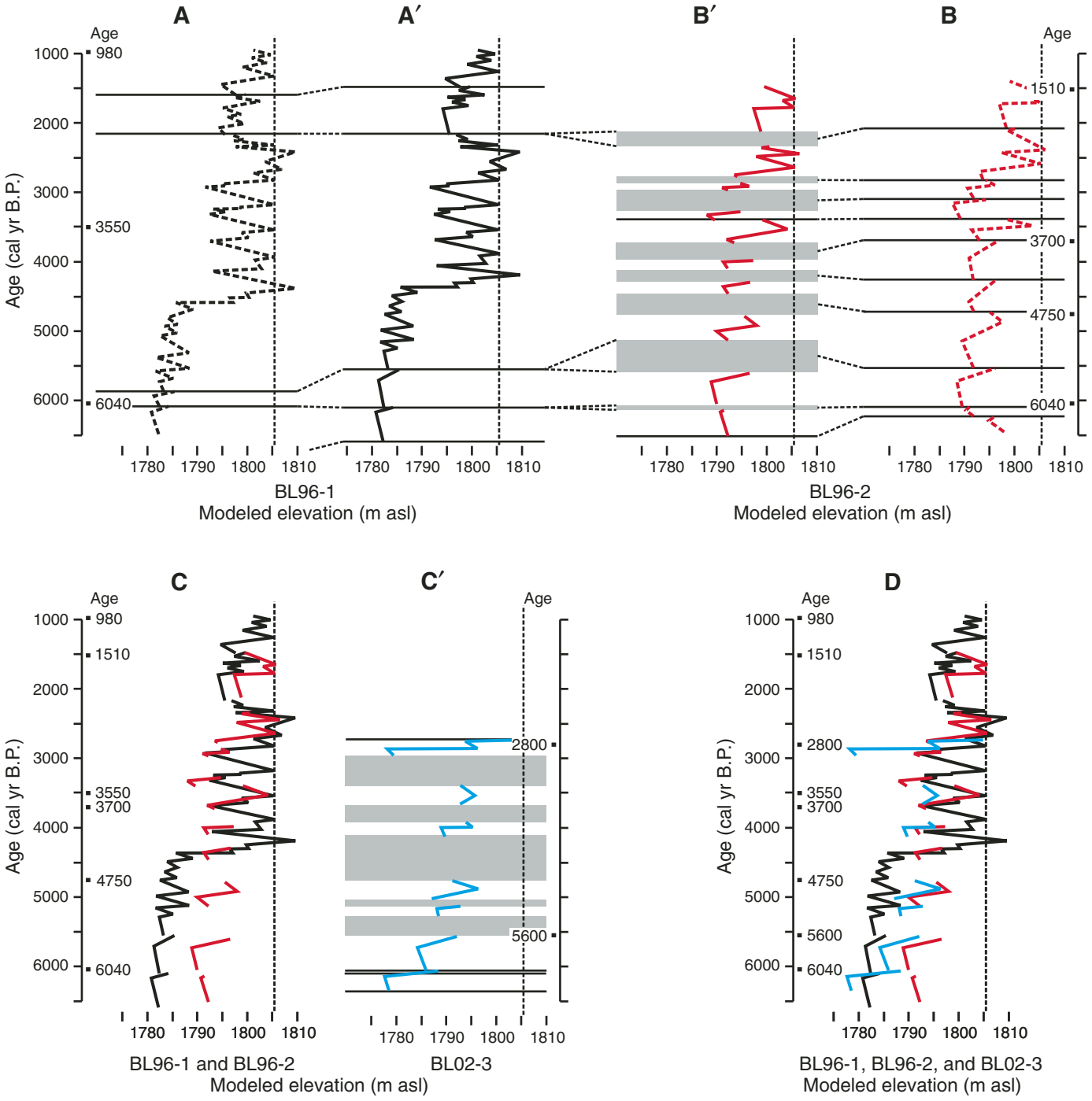

Figure 14. Illustration of method used to produce the alternative chronology for construction of the composite lake-level history (Fig. 16A). Modeled water depths (Fig. 10) have been converted to lake elevation. Portions of the Holocene records (based on sedimentary features) are shown for three cores. Calibrated radiocarbon ages (cal yr B.P.) from Colman et al. (this volume) and their locations are shown to the left or right of age axes. Vertical dashed lines indicate the modern highstand. Horizontal lines signify sharp bedding surfaces (with coarser-grained sediment overlying finer-grained material) that may indicate erosion. (A, B). Unadjusted results for the deepest water site (BL96-1) and the second deepest water site (BL96-2). (A′, B′) Adjusted results for BL96-1 and BL96-2. The curves were adjusted so that lake-level changes are in phase without shifting dated horizons. Erosional gaps (gray bars) were introduced in the shallower record to bring the records into phase and to account for missing fluctuations. Note that erosional surfaces in the deeper record have correlative surfaces in the shallower record. (C, C′). The combined records for BL96-1 and BL96-2 and the adjusted record for next shallower core (BL02-3). The record for BL02-3 was adjusted in the same manner described above. (D) The combined records for BL96-1, BL96-2, and BL02-3. Similar adjustments were made for site BL02-4. asl—above sea level.

The two age models for the siliciclastic interval differ considerably. If the radiocarbon ages are treated in a manner similar to the rest of the core, only two ages fall out of the confidence limits of Colman et al. (this volume): (1) An age of 14,430 cal yr B.P. in BL96-2 is out of order with the other ages. (2) An age of 26,080 cal yr B.P. in BL96-3 is out of order with other dates in that core. Using this correlation, magnetic feature 10 of Colman et al. (this volume) is not the same age in BL96-2 and BL96-3. Because Colman et al. (this volume) discard most of the ages from the siliciclastic interval, it is constrained only by the one age at the base of BL96-3, and by ages overlying rooted horizons that are interpreted as depositional gaps. For the second model, we assumed that the magnetic correlation between cores BL96-3 and BL00-1 by Rosenbaum and Heil (this volume) is correct. We assumed that the sedimentation rates in BL96-3 and BL00-1 were proportional, so that a linear sedimentation trend could be projected through the correlative magnetic features and the two radiocarbon ages in BL00-1 and the one radiocarbon age in BL96-3. Using this approach, the age of the oldest rooted horizon in BL96-3 projects to ca. 20,000 cal yr B.P. We then aligned magnetic feature 10 in BL96-2 to BL96-3, and then matched the silty intervals that are interpreted as indicators of lake-level fluctuations. Assuming a proportional accumulation rate in BL96-2 to the projection of the ages in BL00-1 and BL96-3 produces an age of ca. 19,100 cal yr B.P. for the lowest rooted horizon in BL96-2. The oldest rooted horizon in BL02-4 was assumed to be between the ages at BL96-2 and BL96-3 and the silty intervals were then aligned. The radiocarbon age of 19,370 cal yr B.P. in BL96-2 falls within the confidence interval using this approach. Like Colman et al. (this volume), we rejected the age of 14,430 cal yr B.P. in BL96-2 because it is younger than accepted ages from overlying sediment. If we reject the age of 16,690 cal yr B.P. in BL96-2, the sedimentation interval between the two root horizons is completely unconstrained. Therefore, we accepted this age for lack of any other information.

A comparison of the smoothed age curves of Colman et al. (this volume) to the inferred ages based on the alternative chronology (Fig. 15) shows minor differences. The largest differences are due to the incorporation of erosional breaks and to associated changes in sedimentation rate. In general, the coarser-grained intervals that are attributed to lake-level drops have higher sedimentation rates than the fine-grained intervals attributed to lake-level rises. The largest deviations from the models of Colman et al. (this volume) are in the siliciclastic intervals, even when using the same magnetic correlation and rejected radiocarbon ages. The difference is due to the projection of accumulation rates across rooted horizons by Colman et al. (this volume). One magnetic feature in BL02-4 was not correlated to its presumed match in BL96-2 because the rooted horizons would occur out of sequence.

Composite Lake Level

Based on the alternative chronology, we used the individual core water-depth curves (Fig. 10) to create a composite lake-level curve (Fig. 16A). For the carbonate-rich sediments, grain-size data were used to establish water depth and sedimentary features to indicate changes in lake level. Interpretations based on sedimentary features were favored where grain-size data miss obvious textural changes. In otherwise unconstrained intervals, nonlinear sedimentation rates were used so that similar sediment types had similar relative accumulation rates. For example, transgressive aragonite layers dominated by precipitated crystals had lower accumulation rates than regressive layers dominated by sediment focusing. At Bear Lake, subaerial paleoshorelines are excellent indicators of past lake levels, but the reported ages are inconsistent with ages and interpreted depths from the cores. We suggest that the shoreline ages are too old due to reworking of older shell material and unknown reservoir effects. We interpret the Willis Ranch shoreline (9220 ± 360 cal yr B.P., Table 1) to be equivalent to the upper calcite layer, which is dated several hundred to a thousand years younger. If the published age of the Raspberry Square phase (Table 1) is too old by a similar amount, then it is equivalent to the lowest calcite layer. Similar adjustments in shell ages from Lifton shoreline deposits (Table 1) make the elevation of this shoreline correspond to that of the lake-level rise at 6800 cal yr B.P. The siliciclastic mud intervals are mostly constrained by a spilling lake with little change of depth and by maximum depths suggested by wave-rippled sand in BL2K-2. It was assumed that coarser-grained intervals accumulated more quickly than finer-grained intervals, as suggested by the intervals constrained by radiocarbon ages. The mixed calcitic-siliciclastic mud interval is constrained by the depth of the marsh deposits in BL02-1 and the rooted horizons.

DISCUSSION

The lake-level curve (Fig. 16A) indicates that, prior to ca. 18,000 cal yr B.P., the lake level was stable and subsequently varied radically. This difference is attributed to a change from an older spilling lake to one that was primarily closed. The timing of the first major drop in Bear Lake appears to coincide with the time Lake Bonneville was rising to the Bonneville shoreline (Fig. 16B). If the differences are not due to dating problems in one or both of the records, the diversion of Bear River from Bear Lake may have allowed more water to reach Lake Bonneville without the leakage and evaporation inherent with a period of storage in a lake basin. Lake Bonneville was spilling over its threshold when Bear Lake first became topographically closed. The post-Provo drop in the level of Lake Bonneville roughly corresponds to the 15,000–12,000 cal yr B.P. low lake stand in Bear Lake, and the rise of Lake Bonneville to the Gilbert shoreline at 11,500 cal yr B.P. matches a calcite layer overlying a rooted horizon in Bear Lake. These events occurred after the Bonneville flood, when the lake rapidly dropped from the Bonneville shoreline to the Provo shoreline. The lowstand between ca. 14.8 and 11.8 ka was punctuated by a drop to ~40 m below modern level from ca. 12.8 to 11.8 ka.

For the most part, lake levels at Bear Lake during the Holocene were lower than the historical range of lake levels. Peaks near or above the modern lake occurred at 8500–8000,

7000–6500, 4500–3500, 2500, and 700 cal yr B.P. Rises in the surface of Owens Lake (California) ca. 9000–7500, 4250–3000, and 500 cal yr B.P. (Bacon et al., 2006) roughly coincide with rises of Bear Lake. In addition, Bear Lake high-water periods, except the earliest, roughly correspond to "wetter" intervals at Pyramid Lake (Fig. 16C), although their relative magnitudes differ. In the Owens Lake record (Fig. 16F), there are intervals of increased wetness at 8500, 7700–6500, 2500, and 1000 cal yr B.P. At Bear Lake, levels 15–20 m below the modern highstand occurred ca. 10,000–9000, 7000, 6500–4500, 3500, 3000–2500, 2000, and 1500 cal yr B.P. Each of these dry periods has roughly synchronous "dryer" intervals in the Pyramid Lake and Owens Lake records. The interval of 6500–4500 cal yr B.P. corresponds to a major erosional break with soils at Owens Lake, tree stumps of that age occur below lake level at Lake Tahoe, and during that time the Truckee River stopped flowing to Pyramid Lake (Benson, 2004). The 3000 and 7000 cal yr B.P. lowstands at Bear Lake roughly coincide with dry intervals at Pyramid Lake indicated by a sandy erosional surface in the deep part of the lake (Benson, 2004) and by an isotopically heavy interval, respectively.

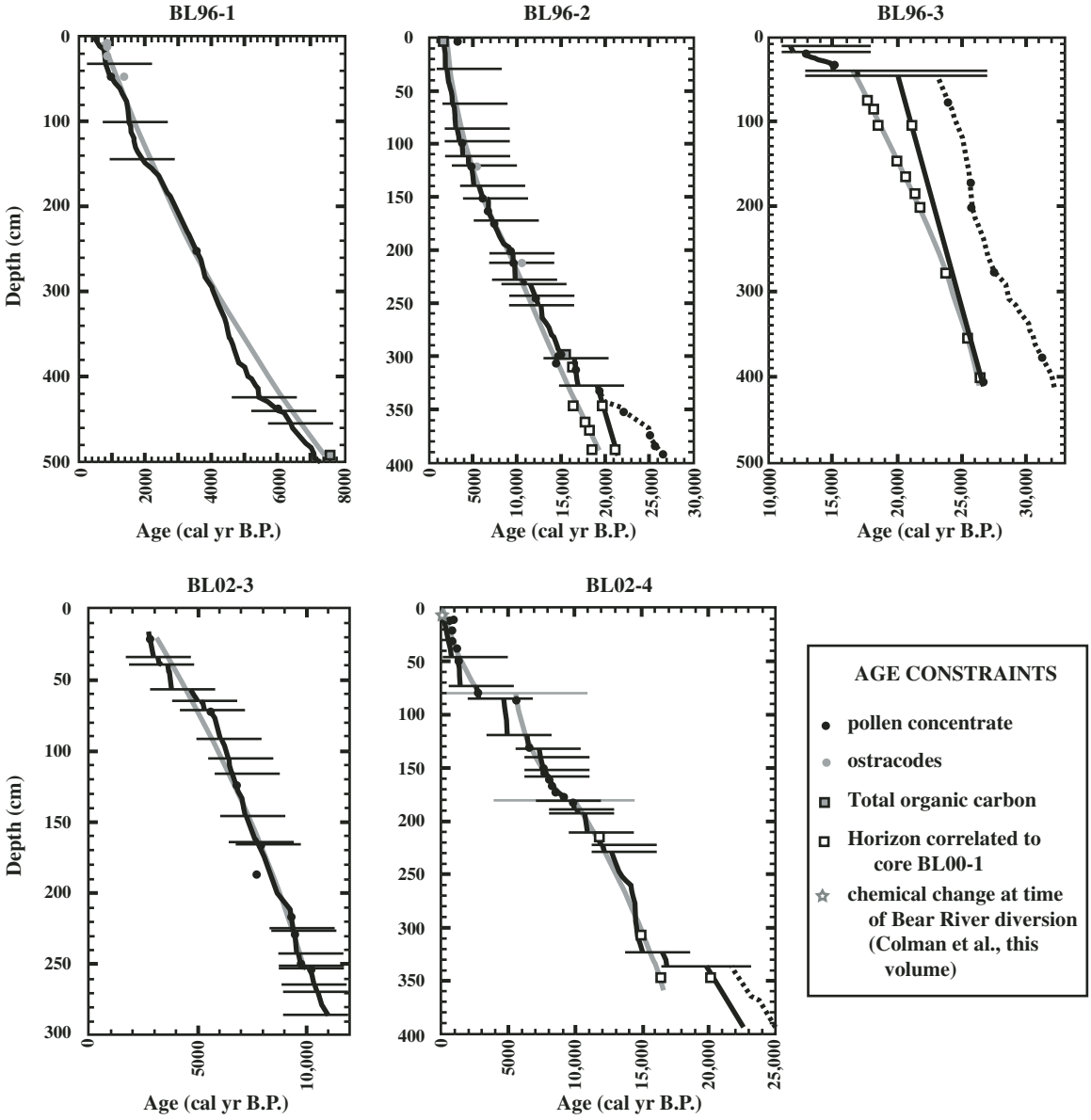

Figure 15. Comparison of age-versus-depth plots using the smoothed age models of Colman et al. (this volume) (heavy gray lines) and the alternative chronology described in the text (heavy black lines). Thin horizontal lines indicate erosional surfaces used in the smoothed age models (gray) and the alternative chronology (black). Dashed black lines indicate the chronology for the siliciclastic interval using the radiocarbon ages versus the solid black lines that assume the radiocarbon ages are too old as in Colman et al. (this volume). Symbols indicate age constraints.

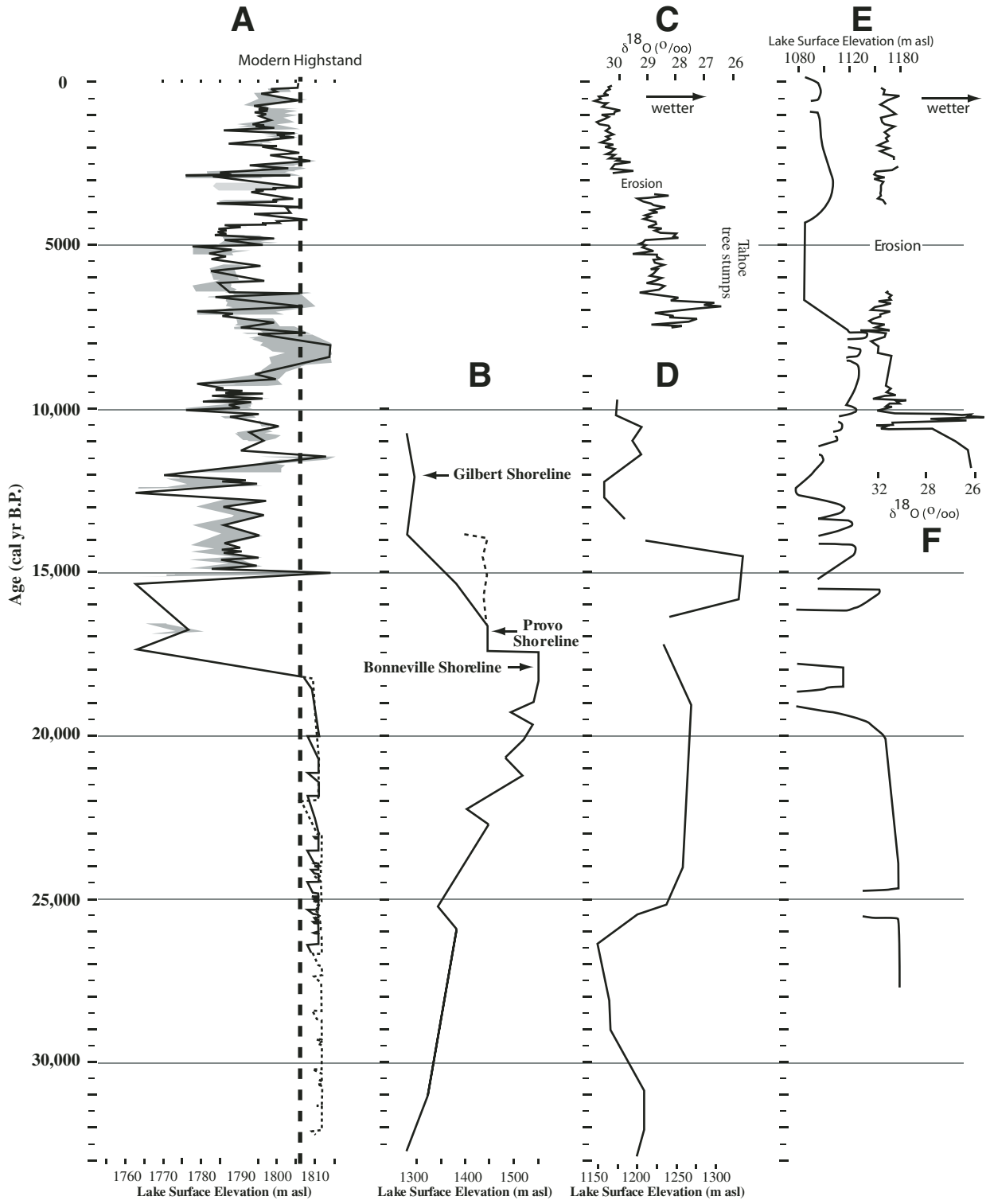

Figure 16. Lake-surface elevation history of Bear Lake compared with surface elevation changes and climate proxies from other lakes. (A) Lake-elevation curve using the alternative chronology. Lake elevations were chosen from the combined data sets using criteria given in text. Gray area shows range of interpretations in the combined data sets. The grain-size data for siliciclastic-rich intervals are not included in that range. Dashed line shows model if radiocarbon ages in the siliciclastic interval that were rejected by Colman et al. (this volume) are used. (B) Lake surface elevations for Lake Bonneville, Utah, based primarily on shoreline dates (modified from Oviatt [1997]). The dashed line indicates an alternative interpretation by Godsey et al. (2005). (C) Oxygen isotope measurements from sediments of Pyramid Lake, Nevada (modified from Benson [2004]). Lighter values are interpreted as higher inflow (wetter). (D) Lake surface elevations for Pyramid Lake, Nevada, based primarily on tufa elevations and ages (modified from Benson [2004]). (E) Lake-surface elevations for Owens Lake. Most ages are from tufa and shells with no reservoir-effect correction (modified from Bacon et al. [2006]). (F) Oxygen isotope measurements from sediments of Owens Lake, California (modified from Benson [2004]). Lower values are interpreted as higher inflow (wetter). asl—above sea level.

The Pleistocene lake-level record at Bear Lake after 18,000 cal yr B.P. is similar to the Pyramid Lake (Fig. 16D) and Owens Lake (Fig. 16E) records. The lowstand at 17,500–15,500 cal yr B.P. at Bear Lake coincides with a lowstand at Pyramid Lake and to a period of erosion and soil development at Owens Lake (Benson, 2004; Bacon et al., 2006). The Owens Lake record indicates that the drop in lake level began earlier than indicated in the Bear Lake record, and that a brief rise in lake level was also earlier. Some of this offset could be due to the uncorrected reservoir effect in dating tufa and shells at Owens Lake. The highstand at 15,000 cal yr B.P. at Bear Lake, correlated with the Raspberry Square phase, roughly equates to the Lahontan highstand at Pyramid Lake; spilling-lake conditions at Owens Lake appear earlier according to the data of Bacon et al. (2006). The lowstand at Bear Lake culminating ca. 12,500 cal yr B.P. corresponds to the drop of Lake Lahontan at Pyramid Lake to the level of the modern closed lake and to a lowstand at Owens Lake. The Bear Lake highstand at 11,500 cal yr B.P. is roughly synchronous with a lake-level rise at Pyramid Lake, although a similar rise is missing in the Owens Lake elevation curve of Bacon et al. (2006). The isotopic data of Benson (2004), however, suggest a period of spilling conditions at that time. The lake-level record at Bear Lake before 18,000 cal yr B.P. does not appear to show any of the variability described from Pyramid Lake or Owens Lake.

SUMMARY

The Bear Lake sedimentary record provides a detailed history of lake-level fluctuations, but some of the age constraints of these changes are less clear. The history of fluctuations was reconstructed by combining three techniques for estimating past water depth. The most clear-cut indicators of lake elevation are shoreline deposits, but they have relatively low preservation potential and are difficult to date. A quantitative lake-level proxy, based on grain-size data from cored sediment, was developed by comparison to modern grain-size distributions. This proxy is best applied to the aragonite sequences most similar to the modern, pre-diversion sediments, and is inappropriate for siliciclastic-rich Pleistocene deposits. Sedimentary textures are sensitive indicators of lake-level fluctuations, but are poorly constrained with respect to actual lake levels. Interpretations of lake-level from sedimentary textures are weakest for deposits with no modern analogs, whose depths of deposition are a matter of speculation. Derivation of a single lake-level history using these three types of data from multiple cores and subaerial exposures required development of an alternative chronology. Smooth age-depth models for Bear Lake cores (Colman et al., this volume) are inadequate because they assume no abrupt changes in sedimentation rate and no gaps in the record. The alternative chronology assumes that the pollen-based radiocarbon ages are mostly correct, that erosional gaps exist in the record, and that gaps are larger in shallower-water deposits than in deeper-water deposits. The lake-level curve produced using the alternative chronology shows some coincidence of lake-level drops and rises with wet and dry intervals at Pyramid Lake and Owens Lake, particularly during the past 8000 years. The Lake Bonneville record is less coincident with that of Bear Lake. The Bonneville highstand occurred during a Bear Lake lowstand that followed diversion of the Bear River away from the basin. The Bear Lake lowstand may have occurred during a major drought that was not recorded in the Bonneville Basin because it was a spilling lake.

The approach of using combined sedimentological constraints on lake levels should be applicable to most lakes. Shoreline data will be most useful in settings with high clastic sediment input, varied sources of material suitable for dating, and a range of slopes within the basin. Grain-size data will be most useful if the basin floor is very flat. Best results will come from lakes with large areas well removed from river mouths and a continuous record with no changes in provenance. The range of sedimentary textures will vary with each lake basin and will have to be evaluated for that basin. Closed-basin drainages are much more variable in depth and area, providing more contrast in sedimentary features than is found in spilling lakes.

ARCHIVED DATA

Archived data for this chapter can be obtained from the NOAA World Data Center for Paleoclimatology at http://www.ncdc.noaa.gov/paleo/pubs/gsa2009bearlake/.

REFERENCES CITED

Adams, K.D., and Wesnousky, S.G., 1998, Shoreline processes and the age of the Lake Lahontan highstand in the Jessup Embayment, Nevada: Geological Society of America Bulletin, v. 110, p. 1318–1332, doi: 10.1130/0016-7606(1998)110<1318:SPATAO>2.3.CO;2.

Bacon, S.N., Burke, R.M., Pezzopane, S.K., and Jayko, A.S., 2006, Last glacial maximum and Holocene lake levels of Owens Lake, eastern California, USA: Quaternary Science Reviews, v. 25, p. 1264–1282, doi: 10.1016/j.quascirev.2005.10.014.

Benson, L.V., 1994, Carbonate deposition, Pyramid Lake Subbasin, Nevada: 1. Sequence of formation and elevational distribution of carbonate deposits (tufas): Palaeogeography, Palaeoclimatology, Palaeoecology, v. 109, p. 55–87, doi: 10.1016/0031-0182(94)90118-X.

Benson, L.V., 2004, Western Lakes, *in* Gillespie, A.R., Porter, S.C., and Atwater, B.F., eds., The Quaternary Period in the United States: Amsterdam, Elsevier, Developments in Quaternary Science, v. 1, p. 185–204.

Bjorck, S., and Wohlfarth, B., 2001, ^{14}C chronostratigraphic techniques in paleolimnology, *in* Last, W.M., and Smol, J.P., eds., Tracking environmental change using lake sediments, Volume 1: Basin analysis, coring, and chronological techniques: Dordrecht, Kluwer Academic Publishers, p. 205–245.

Blais, J.M., and Kalff, J., 1995, The influence of lake morphometry on sediment focusing: Limnology and Oceanography, v. 40, p. 582–588.

Broecker, W.S., and Walton, A.F., 1959, The geochemistry of ^{14}C in freshwater systems: Geochimica et Cosmochimica Acta, v. 16, p. 15–38, doi: 10.1016/0016-7037(59)90044-4.

Clifton, H.E., 1976, Wave-formed sedimentary structures: A conceptual model, *in* Davis, R.A., Jr., and Ethington, R.L., eds., Beach and nearshore sedimentation: Tulsa, Oklahoma, SEPM Special Publication 24, p. 126–148.

Coleman, J.M., 1981, Deltas: Processes and Models for Exploration: Minneapolis, Burgess Publication Co., 124 p.

Colman, S.M., 2006, Acoustic stratigraphy of Bear Lake, Utah-Idaho—Late Quaternary sedimentation patterns in a simple half-graben: Sedimentary Geology, v. 185, p. 113–125, doi: 10.1016/j.sedgeo.2005.11.022.

Colman, S.M., Rosenbaum, J.G., Kaufman, D.S., Dean, W.E., and McGeehin, J.P., 2009, this volume, Radiocarbon ages and age models for the past 30,000 years in Bear Lake, Utah and Idaho, *in* Rosenbaum, J.G., and

Kaufman, D.S., eds., Paleoenvironments of Bear Lake, Utah and Idaho, and its catchment: Geological Society of America Special Paper 450, doi: 10.1130/2009.2450(05).

Davis, M.B., and Ford, M.S., 1982, Sediment focusing in Mirror Lake, New Hampshire: Limnology and Oceanography, v. 27, p. 137–150.

Dean, W.E., 2009, this volume, Endogenic carbonate sedimentation in Bear Lake, Utah and Idaho, over the last two glacial-interglacial cycles, *in* Rosenbaum, J.G., and Kaufman, D.S., eds., Paleoenvironments of Bear Lake, Utah and Idaho, and its catchment: Geological Society of America Special Paper 450, doi: 10.1130/2009.2450(07).

Dean, W., Rosenbaum, J., Skipp, G., Colman, S., Forester, R., Liu, A., Simmons, K., and Bischoff, J., 2006, Unusual Holocene and late Pleistocene carbonate sedimentation in Bear Lake, Utah and Idaho, USA: Sedimentary Geology, v. 185, p. 93–112, doi: 10.1016/j.sedgeo.2005.11.016.

Dean, W.E., Wurtsbaugh, W.A., and Lamarra, V.A., 2009, this volume, Climatic and limnologic setting of Bear Lake, Utah and Idaho, *in* Rosenbaum, J.G., and Kaufman, D.S., eds., Paleoenvironments of Bear Lake, Utah and Idaho, and its catchment: Geological Society of America Special Paper 450, doi: 10.1130/2009.2450(01).

Denny, J.F., and Colman, S.M., 2003, Geophysical surveys of Bear Lake, Utah-Idaho, September 2002: U.S. Geological Survey Open-File Report 03-150.

Gilbert, G.K., 1885, The topographic features of lake shores: U.S. Geological Survey, Firth Annual Report, p. 69–123.

Godsey, H.S., Currey, D.R., and Chan, M.A., 2005, New evidence for an extended occupation of the Provo Shoreline and implications for regional climate change, Pleistocene Lake Bonneville, Utah, USA: Quaternary Research, v. 63, p. 212–223, doi: 10.1016/j.yqres.2005.01.002.

Hakanson, L., 1977, The influence of wind, fetch, and water depth on distribution of sediments in Lake Vanern, Sweden: Canadian Journal of Earth Sciences, v. 14, p. 397–412.

Hakanson, L., 1982, Lake bottom dynamics and morphometry: The dynamic ratio: Water Resources Research, v. 18, p. 1444–1450, doi: 10.1029/WR018i005p01444.

Hakanson, L., 1995, Models to predict net and gross sedimentation in lakes: Marine and Freshwater Research, v. 46, p. 305–319.

Hakanson, L., and Jansson, M., 1983, Principles of lake sedimentology: Berlin, Springer-Verlag, 316 p.

Harms, J.C., Southard, J.B., and Walker, R.G., 1982, Structures and sequences in clastic rocks: Tulsa, Oklahoma, SEPM Short Course no. 9, 249 p.

Hasiotis, S.T., 2002, Continental trace fossils: Tulsa, Oklahoma, SEPM Short Course Notes no. 51, 132 p.

Hilton, J., 1985, A conceptual framework for predicting the occurrence of sediment focusing and sediment redistribution in lakes: Limnology and Oceanography, v. 30, p. 1131–1143.

Hutchinson, G.E., 1975, Limnological botany, v. 3 of A treatise on limnology: New York, John Wiley and Sons, 660 p.

Johnson, T.C., 1980, Sediment redistribution by waves in lakes, reservoirs, and embayments, *in* Proceedings, Symposium on Surface Water Impoundments, Minneapolis, June 1980: Minneapolis, American Society of Civil Engineers, p. 1307–1317.

Kaufman, D.S., Bright, J., Dean, W.E., Rosenbaum, J.G., Moser, K., Anderson, R.S., Colman, S.M., Heil, C.W., Jr., Jiménez-Moreno, G., Reheis, M.C., and Simmons, K.R., 2009, this volume, A quarter-million years of paleoenvironmental change at Bear Lake, Utah and Idaho, *in* Rosenbaum, J.G., and Kaufman, D.S., eds., Paleoenvironments of Bear Lake, Utah and Idaho, and its catchment: Geological Society of America Special Paper 450, doi: 10.1130/2009.2450(14).

Komar, P.D., 1998, Beach processes and sedimentation (2nd edition): Upper Saddle River, New Jersey, Prentice Hall, 544 p.

Komar, P.D., and Miller, M.C., 1973, The threshold of sediment movement under oscillatory water waves: Journal of Sedimentary Petrology, v. 43, p. 1101–1110.

Komar, P.D., and Miller, M.C., 1975, On the comparison between the threshold of sediment motion under waves and unidirectional currents with a discussion on the practical evaluation of the threshold: Journal of Sedimentary Petrology, v. 45, p. 362–367.

Laabs, B.J.C., 2001, Quaternary lake-level history and tectonic geomorphology of Bear Lake Valley, Utah and Idaho [M.S. thesis]: Flagstaff, Northern Arizona University, 132 p.

Laabs, B.J.C., and Kaufman, D.S., 2003, Quaternary highstands in Bear Lake Valley, Utah and Idaho: Geological Society of America Bulletin, v. 115, p. 463–478, doi: 10.1130/0016-7606(2003)115<0463:QHIBLV>2.0.CO;2.

Lehman, J.T., 1975, Reconstructing the rate of accumulation of lake sediment: The effect of sediment focussing: Quaternary Research, v. 5, p. 541–550, doi: 10.1016/0033-5894(75)90015-0.

McCalpin, J.P., 1993, Neotectonics of the northeastern Basin and Range margin, western U.S.A.: Zeitschrift für Geomorphologie, N.F., Suppl. Bd., v. 94, p. 137–157.

Moser, K.A., and Kimball, J.P., 2009, this volume, A 19,000-year record of hydrologic and climatic change inferred from diatoms from Bear Lake, Utah and Idaho, *in* Rosenbaum, J.G., and Kaufman, D.S., eds., Paleoenvironments of Bear Lake, Utah and Idaho, and its catchment: Geological Society of America Special Paper 450, doi: 10.1130/2009.2450(10).

Nemec, W., 1995, The dynamics of deltaic suspension plumes, *in* Ori, M.N., and Postma, G., eds., Geology of deltas: Rotterdam, A.A. Balkema, p. 31–93.

Olsson, I., 1986, Radiometric dating, *in* Berglund, B.E., ed., Handbook of Holocene palaeoecology and palaeohydrology: New York, John Wiley and Sons, p. 273–312.

Oviatt, C.G., 1997, Lake Bonneville fluctuations and global climate change: Geology, v. 25, p. 155–158, doi: 10.1130/0091-7613(1997)025<0155:LBFAGC>2.3.CO;2.

Reheis, M.C., Laabs, B.J.C., Forester, R.M., McGeehin, J.P., Kaufman, D.S., and Bright, J., 2005, Surficial deposits in the Bear Lake Basin: U.S. Geological Survey Open-File Report 2005-1088, 30 p.

Reheis, M.C., Laabs, B.J.C., and Kaufman, D.S., 2009, this volume, Geology and geomorphology of Bear Lake Valley and upper Bear River, Utah and Idaho, *in* Rosenbaum, J.G., and Kaufman, D.S., eds., Paleoenvironments of Bear Lake, Utah and Idaho, and its catchment: Geological Society of America Special Paper 450, doi: 10.1130/2009.2450(02).

Robertson, G.C., 1978, Surficial deposits and geologic history, northern Bear Lake, Idaho [M.S. thesis]: Logan, Utah State University, 162 p.

Rosenbaum, J.G., and Heil, C.W., Jr., 2009, this volume, The glacial/deglacial history of sedimentation in Bear Lake, Utah and Idaho, *in* Rosenbaum, J.G., and Kaufman, D.S., eds., Paleoenvironments of Bear Lake, Utah and Idaho, and its catchment: Geological Society of America Special Paper 450, doi: 10.1130/2009.2450(11).

Rosenbaum, J.G., Dean, W.E., Reynolds, R.L., and Reheis, M.C., 2009, this volume, Allogenic sedimentary components of Bear Lake, Utah and Idaho, *in* Rosenbaum, J.G., and Kaufman, D.S., eds., Paleoenvironments of Bear Lake, Utah and Idaho, and its catchment: Geological Society of America Special Paper 450, doi: 10.1130/2009.2450(06).

Rowan, D.J., Kalff, J., and Rasmussen, J.B., 1992, Estimating the mud deposition boundary depth in lakes from wave theory: Canadian Journal of Fisheries and Aquatic Sciences, v. 49, p. 2490–2497, doi: 10.1139/f92-275.

Smith, N.D., and Ashley, G., 1985, Proglacial lacustrine environment, *in* Ashley, G., Shaw, J., and Smith, N.D., eds., Glacial sedimentary environments: Tulsa, Oklahoma, SEPM Special Publication 16, p. 135–216.

Smoot, J.P., 2003, Impact of sedimentation styles on paleoclimate proxies in late Pleistocene through Holocene lakes in the western U.S.: International Limnogeology Congress, 3rd, Tucson, Abstracts, p. 273.

Smoot, J.P., 2009, this volume, Late Quaternary sedimentary features of Bear Lake, Utah and Idaho, *in* Rosenbaum, J.G., and Kaufman, D.S., eds., Paleoenvironments of Bear Lake, Utah and Idaho, and its catchment: Geological Society of America Special Paper 450, doi: 10.1130/2009.2450(03).

Smoot, J.P., and Lowenstein, T.K., 1991, Depositional environments of non-marine evaporites, *in* Melvin, J.L., ed., Evaporites, petroleum and mineral resources: Elsevier, Amsterdam, Developments in Sedimentology, v. 50, p. 189–347.

Smoot, J.P., and Benson, L.V., 1998, Sedimentary structures as indicators of paleoclimatic fluctuations, Pyramid Lake, Nevada, *in* Pitman, J.K., and Carroll, A.R., eds., Modern and ancient lake systems: Salt Lake City, Utah Geological Association, Guidebook 26, p. 131–161.

Smoot, J.P., and Benson, L.V., 2004, Mechanical mixing of climate proxies by sediment focusing in Pyramid Lake, Nevada: A cautionary tale: Geological Society of America Abstracts with Programs, v. 36, no. 5, p. 473.

Stuiver, M., Reimer, P.J., and Braziunas, T.F., 1998, High-precision radiocarbon age calibration for terrestrial and marine samples: Radiocarbon, v. 40, p. 1127–1151.

Sturm, M., 1979, Origin and composition of clastic varves, *in* Schluchter, C., ed., Moraines and varves: Rotterdam, A.A. Balkema, p. 281–285.

Williams, J.S., Willard, A.D., and Parker, V., 1962, Recent history of Bear Lake Valley, Utah-Idaho: American Journal of Science, v. 260, p. 24–36.

Manuscript Accepted by the Society 15 September 2008

Printed in the USA

Sedimentary constraints on late Quaternary lake-level fluctuations at Bear Lake, Utah and Idaho

Joseph P Smoot and Joseph G Rosenbaum

Geological Society of America Special Papers 2009;450; 263-290
doi:10.1130/2009.2450(12)